2. Interaction of particles and matter

2.1. Energy loss by ionisation (heavy particle)
2.2. Interaction of photons
2.3. Interaction of electrons
- Ionisation
- Bremsstrahlung

2.4. Cherenkov effect
2.5. Transition radiation

- very compact presentation, since material should be largely known
- but some additional material, units, useful relations
- more emphasis on some aspects that are new beyond Physics V and important for detectors

good, but very compact presentation of material, including many references in
→ Review of Particle Physics, Phys. Lett. B667 (2008) p.267 -
"Passage of radiation through matter" by Bichsel, Groom, Klein

2.1. Energy loss by ionisation   dE/dx

assume $Mc^2 \gg m_e c^2$

Coulomb interaction between particle X and atom

cross section dominated by inelastic collisions with electrons

atom$^+$ + e$^-$ + X   ionisation

atom* + X   excitation

↳ atom + γ

(for electrons also bremsstrahlung, see below)

classical derivation: Bohr 1913

quantum mechanical derivation: H. Bethe Ann. d. Physik 5 (1930) 325   and
F. Bloch, Ann. d. Physik 16 (1933) 285

- **Bohr:** particle with charge ze moves with velocity v through medium with electron density n, electrons considered free and, during collision, at rest

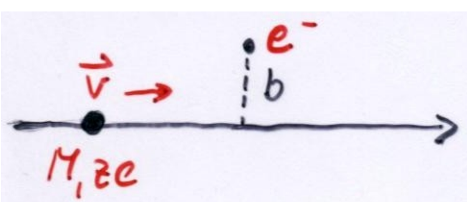

$\Delta p_\perp = \Delta p = \dfrac{2ze^2}{bv}$ $\Delta p_\parallel$ averages to zero

$\Delta E(b) = \dfrac{\Delta p^2}{2m_e}$ energy transfer onto one electron at distance b

per pathlength dx in distance between b and b + db $n2\pi b\,db\,dx$ electrons are found

$$-dE(b) = \frac{n\, 4\pi z^2 e^4}{m_e v^2} \frac{db}{b} dx$$

diverges for b → 0 Bohr: choose relevant range $b_{min} - b_{max}$

$\boxed{b_{min}}$ relative to heavy particle electron is located only within the Broglie wavelength

$$\rightarrow b_{min} = \frac{\hbar}{p} = \frac{\hbar}{\gamma m_e v}$$

$\boxed{b_{max}}$ duration of perturbation (interaction time) shorter than period of electron $\frac{b}{v} \lesssim \frac{\gamma}{\langle\nu\rangle}$

insert and integrate over b $\rightarrow b_{max} = \frac{\gamma v}{\langle\nu\rangle}$

$$\boxed{-\frac{dE}{dx} = \frac{4\pi z^2 e^4}{m_e c^2 \beta^2}\, n \ln \frac{m_e c^2 \beta^2 \gamma^2}{\hbar\langle\nu\rangle}}$$

electron density $n = \frac{N_A \cdot \rho \cdot Z}{A}$

average revolution frequency of electron ‹ν› <-> effective ionisation potential I = h ‹ν›

note: here and in the following **e^2 = 1.44 MeV fm** (contains $4\pi\varepsilon_0$)

- **Bethe – Bloch equation**

  considering quantum mechanical effects

$$\boxed{-\frac{dE}{dx} = K z^2 \frac{Z}{A}\rho\frac{1}{\beta^2}\left[\frac{1}{2}\ln\frac{2m_e c^2\beta^2\gamma^2 T_{max}}{I^2} - \beta^2 - \frac{\delta}{2}\right]}$$

$K/A = 4\pi N_A r_e^2 m_e c^2/A$ with classical electron radius $r_e = \frac{e^2}{m_e c^2}$

T_{max} max. energy transfer in a single collision

$\cong 2\, m_e c^2\beta^2\gamma^2$ for $M \gg m_e$

mean excitation energy $I = (10 \pm 1) \cdot Z$ eV for elements beyond oxygen

$\boxed{\text{Density correction} \quad \delta/2}$ (see Jackson)

with increasing particle energy -> Lorentz contraction of electric field, corresponding increase of contribution from large b with $\ln \beta\gamma$

but: real media are polarized, effectively cuts off long range contributions to logarithmic rise

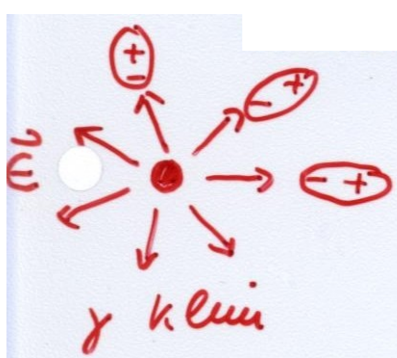

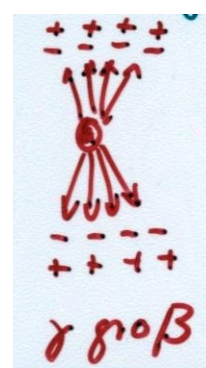

high energy limit $\boxed{\delta/2 \to \ln\left(\frac{\hbar\omega_p}{I}\right) + \ln\beta\gamma - 1/2}$

with plasma energy $\hbar\omega_p = \sqrt{(4\pi n r_e^{\,3})}\, m_e c^2/\alpha$

$\rightarrow$ $-$ dE/dx increases more like ln $\beta\gamma$ than ln $\beta^2\gamma^2$
and I should be replaced by plasma energy

remark: plasma energy $\propto \sqrt{n}$,
i.e. correction much larger
for liquids and solids

one more (small) correction:
shell correction -> for $\beta c \cong v_e$
capture processes possible

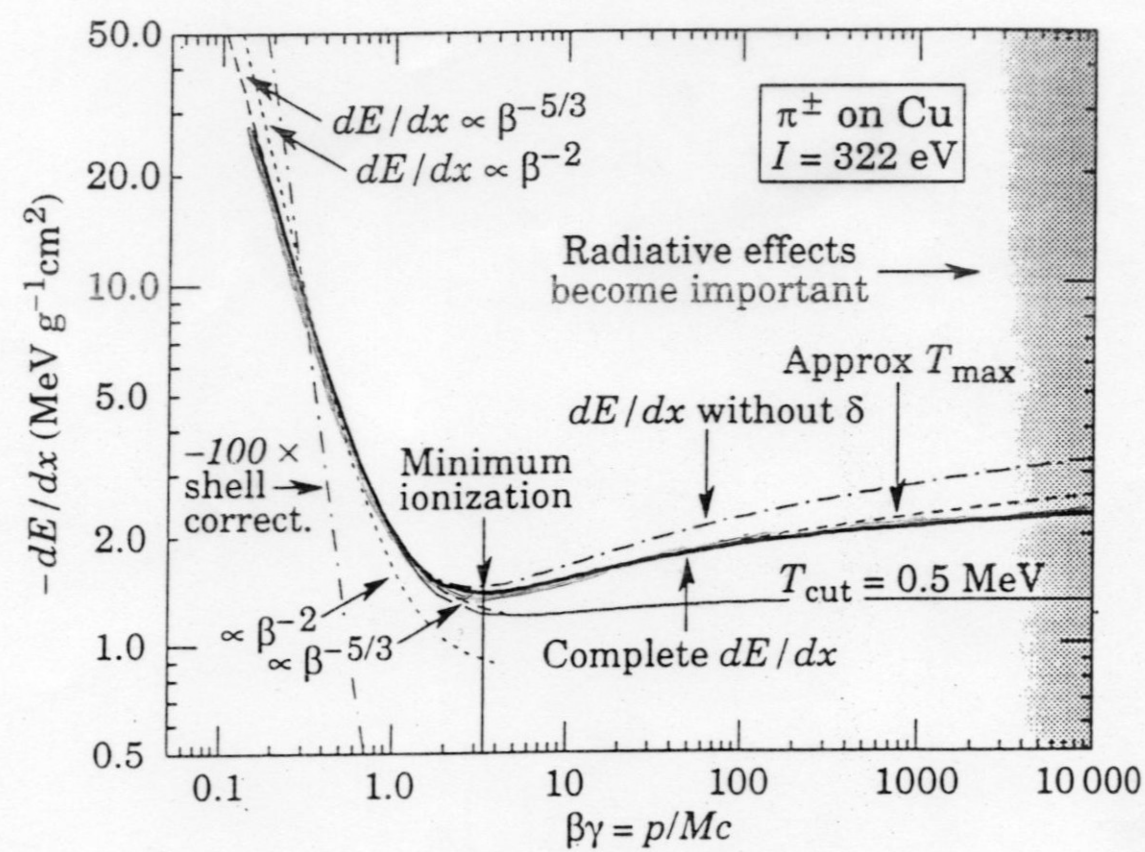

Figure 22.1: Energy loss rate in copper. The function without the density effect correction is also shown, as is the shell correction and two low-energy approximations.

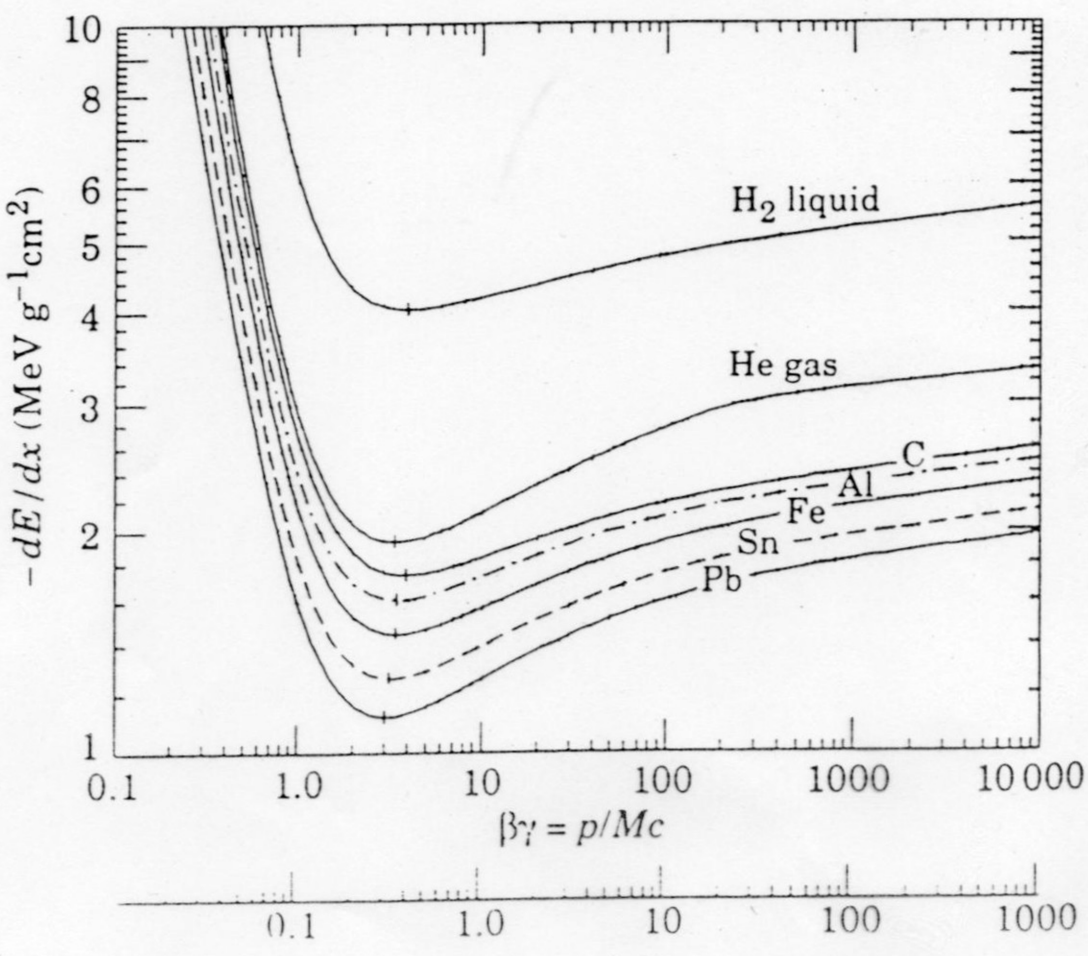

10
8
6
5
4
3
2
1
$-dE/dx$ (MeV g^{-1}cm^2)
H_2 liquid
He gas
C
Al
Fe
Sn
Pb
0.1
1.0
10
100
1000
10 000
$\beta\gamma = p/Mc$
0.1
1.0
10
100
1000

General behavior of dE/dx:

- at low energies/velocities decrease as approx. $\beta^{-5/3}$ up to $\beta\gamma > 1$
- broad minimum at $\beta\gamma \cong 3.5$ $(Z = 7)$ $\big\}\ 1\text{-}2\ \frac{\mathrm{MeV\,cm^2}}{g}$

  3.0 (100)

  "minimally ionising particle"
- logarithmic rise and "Fermi-plateau"

  cut off for very high energy transfer to a few electrons (treated explicitly) T_{cut}

  log. rise 10 % liquids 50% gases
- very low velocities ($v < v_{electron}$ cannot be treated this way)

  for $10^{-3} \leq \beta \leq \alpha \cdot z$ $-dE/dx \propto \beta$ non-ionising, recoil of atomic nuclei

  for $\beta \cdot c \cong v_e$ also capture processes important (shell correction)

2.1.2 Range

Integration over changing energy loss from initial kinetic energy E down to zero

$$R = \int_E^0 \frac{dE}{dE/dx}$$

$\boxed{\text{Abb. R}}$ $\Rightarrow$

MEAN RANGE AND ENERGY LOSS

Mean Range and Energy Loss in Lead, Copper, Aluminum, and Carbon

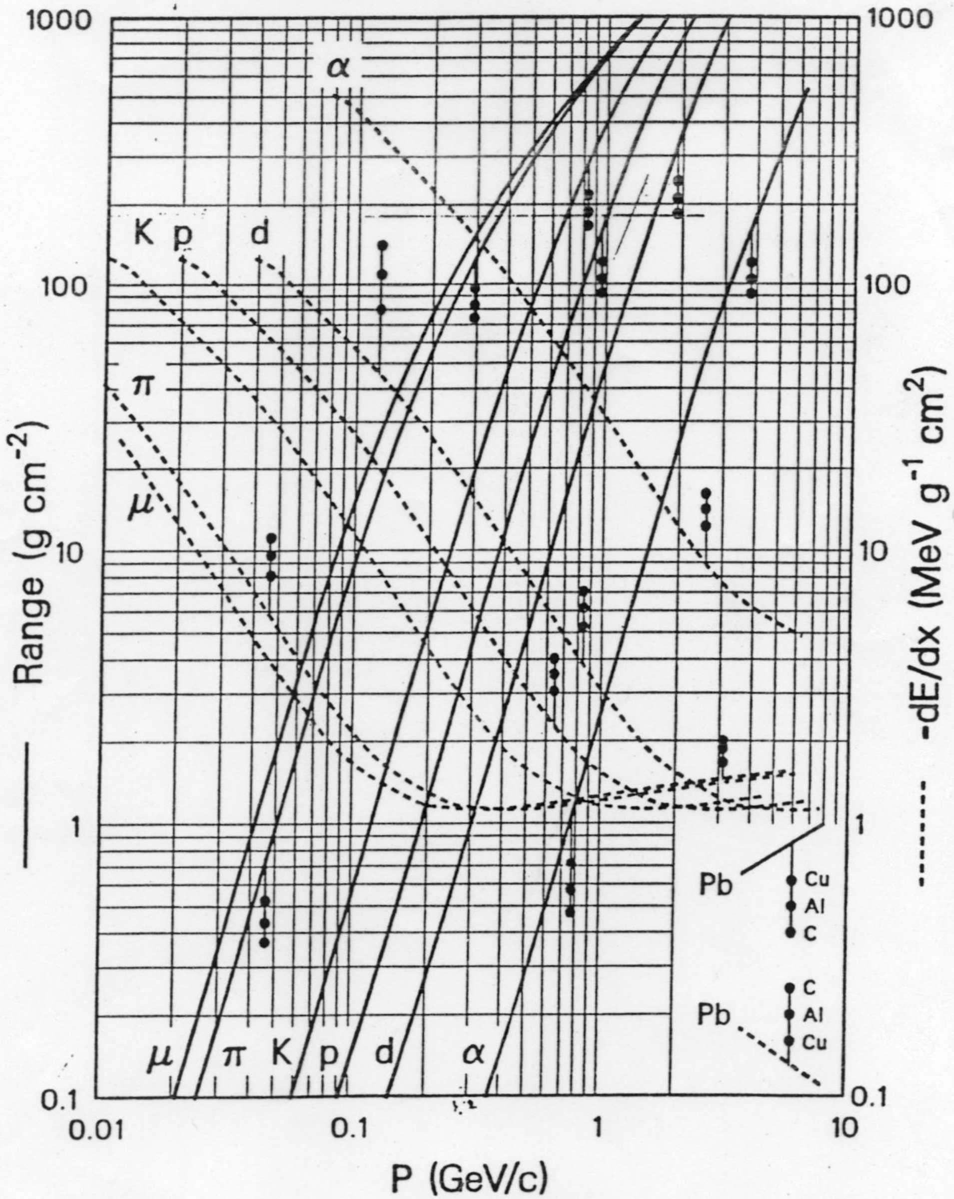

Mean range and energy loss due to ionization for the indicated particles in Pb, with scaling to Cu, Al, and C indicated, using Bethe-Bloch equation [See Sec. (1) of Passage of Particles Through Matter] with corrections. Calculated by M.J. Berger, using ionization potentials and density effect corrections as discussed in M.J. Berger and S.M. Seltzer, "Stopping Powers and Ranges of Electrons and Positrons," (2nd ed.), U.S. National Bureau of Standards Report NBSIR 82-2550-A (1982). The average ionization potentials (I) assumed were: Pb (823 eV), Cu (322 eV), Al (166 eV), and C (78.0 eV). Figure indicates total path length; observed range may be smaller (by ~ 1 % - 2% in heavy elements) due to multiple scattering, primarily from small energy-loss collisions with nuclei. The functional forms have not been experimentally verified to better than roughly ± 1%. For higher energies refer to discussion by Cobb ["A Study of Some Electromagnetic Interactions of High Velocity Particles with Matter," University of Oxford Report HEP/T/55 (1973)] and by Turner ["Penetration of Charged Particles in Matter: A Symposium," National Academy of Sciences, Washington D.C. (1970), p. 48]. For lower energies both data and theory are not well understood. Scaling to other beam particles is, to a good approximation, described by the formula on the next page.

Energy deposition of particles stopped in medium:

for $\beta\gamma \geq 3.5$ $\left\langle \frac{dE}{dx} \right\rangle \simeq \frac{dE}{dx}_{min}$

for $\beta\gamma \geq 3.5$ steep rise $\left\langle \frac{dE}{dx} \right\rangle \gg \frac{dE}{dx}_{min}$ down to very small energies, then decrease again

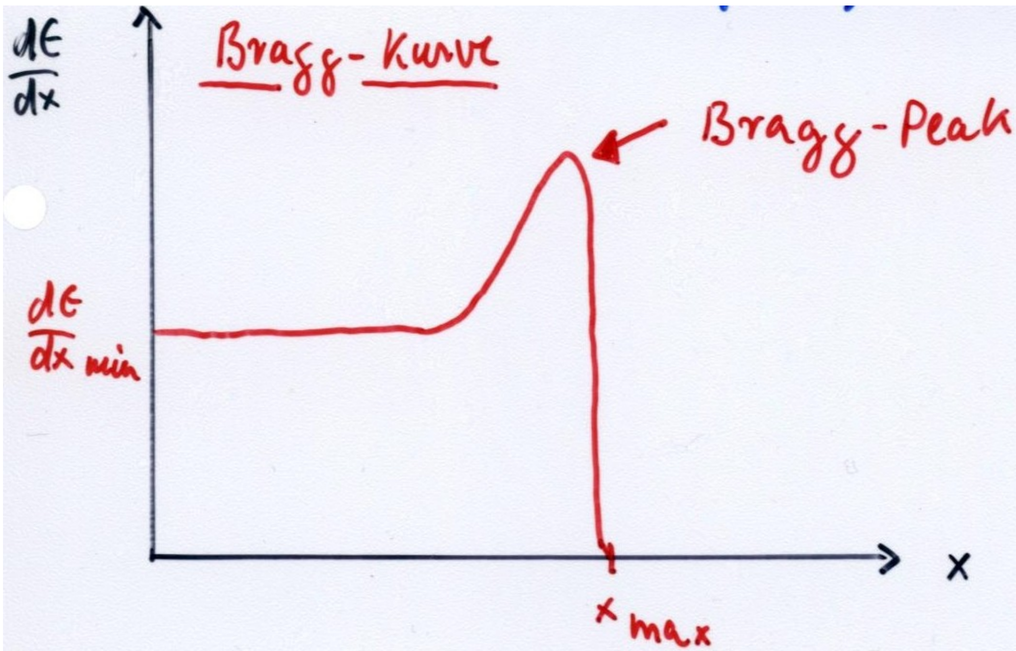

application: tumor therapy – one can deposit precise dose in well defined depth of material (body), determined by initial beam energy

historically protons

in last years also heavy ions, in particular C; presently a tumor centre is being built in Heidelberg (collaboration DKFZ & GSI)

precise 3d irradiation profile by suitably shaped absorber (custom made for each patient)

2.1.3. Delta – electrons

Electrons liberated by ionisation having an energy in excess of some value (e.g. T_{cut}) are called δ – electrons (initial observation in emulsions, hard scattering → energetic electrons)

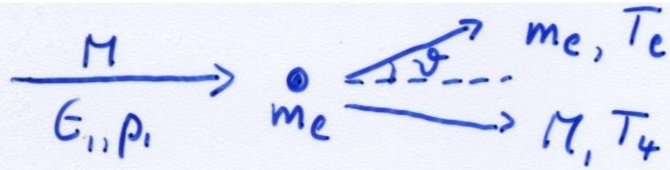

$$T_e = 2 m_e \frac{\vec{p}_1^{\,2} \cos^2\vartheta}{(E_1 + m_e)^2 - \vec{p}_1^{\,2} \cos^2\vartheta} \sim T_e^{max} = \frac{2 m_e \vec{p}_1^{\,2}}{(E_1 + m_e)^2 - \vec{p}_1^{\,2}}$$

für $|\vec{p}_1| \gg M, m_e$

$$T_e^{max} \approx \frac{2 m_e c^2 \beta^2 \gamma^2}{1 + 2\frac{m_e \gamma}{M} + \left(\frac{m_e}{M}\right)^2}$$

Massive highly relativistic particle can transfer practically all its energy to a single electron!
probability distribution for energy transfer E to a single electron

$$\frac{d^2 w}{dx\, dE} = 2 m_e c^2 \pi r_e^2 \frac{z^2}{\beta^2} \cdot \frac{Z}{A} N_A \cdot \rho \cdot \frac{1}{E^2}$$

unpleasant: often this electron is not detected as part of the ionisation trail,
broadening of track and of energy loss distribution

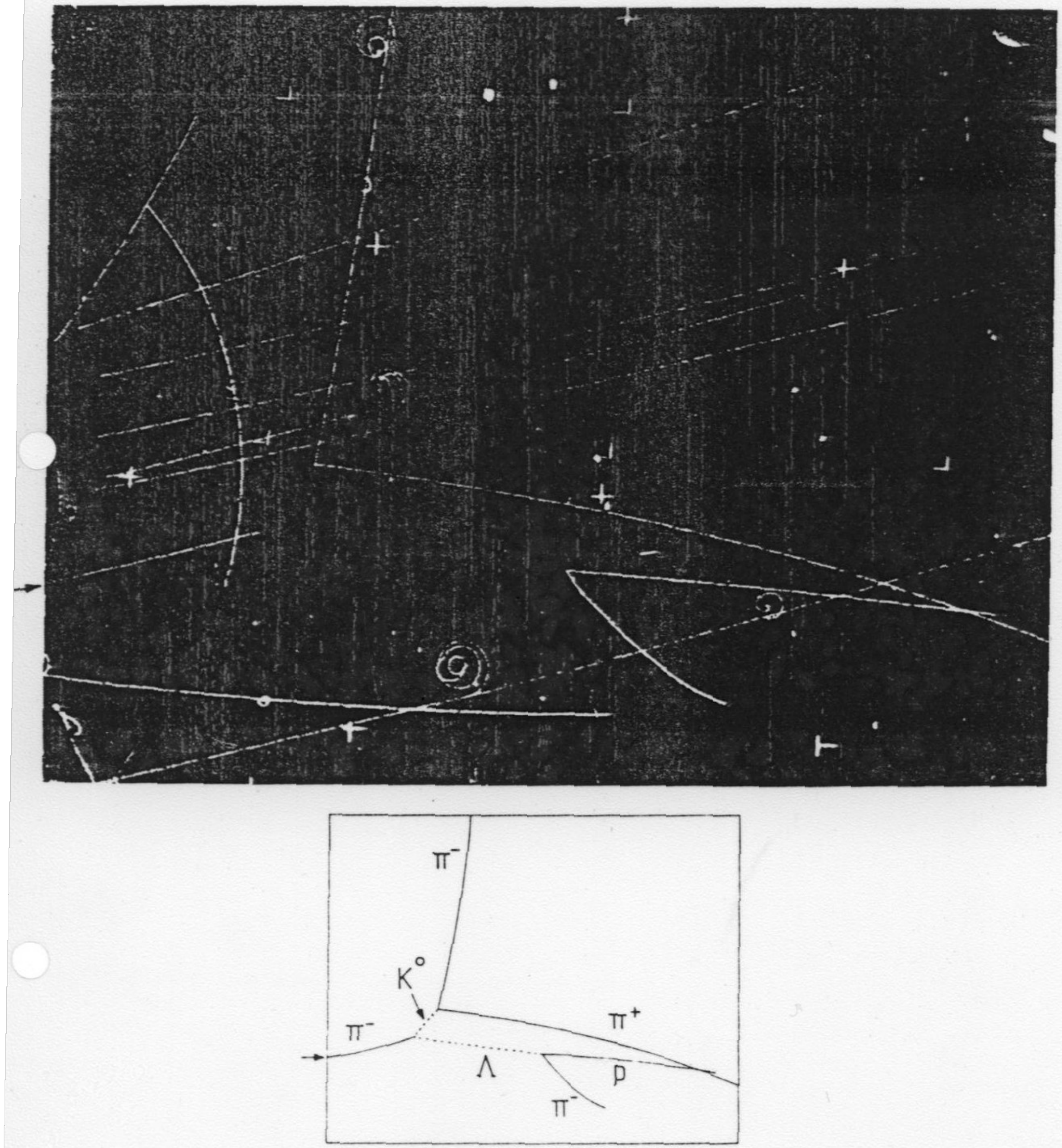

Fig. 2.7 A bubble chamber picture of the associated production reaction $\pi^- + p \rightarrow K^0 + \Lambda$. The incoming pion is indicated by the arrow, and the unseen neutrals are detected by their decays $K^0 \rightarrow \pi^+ + \pi^-$ and $\Lambda \rightarrow \pi^- + p$. This picture was taken in the 10 inch (25 cm) bubble chamber at the Lawrence Berkeley Radiation Laboratory. (Photograph courtesy of the Lawrence Berkeley Radiation Laboratory.)

2.1.4. Energy loss distribution for finite absorber thickness

Energy loss by ionisation is distributed statistically “energy loss straggling”
Bethe-Bloch formula describes the mean energy loss
strong fluctuations about mean: first considered by Bohr 1915 $\sigma^2 = \langle E^2 \rangle - E_0^{\,2} \cong 4\pi n z^2 e^4 \Delta x$

standard deviation of Gauss distribution with mean energy loss E_0

and tail towards high energies due to δ-electrons (actual solution complicated problem)

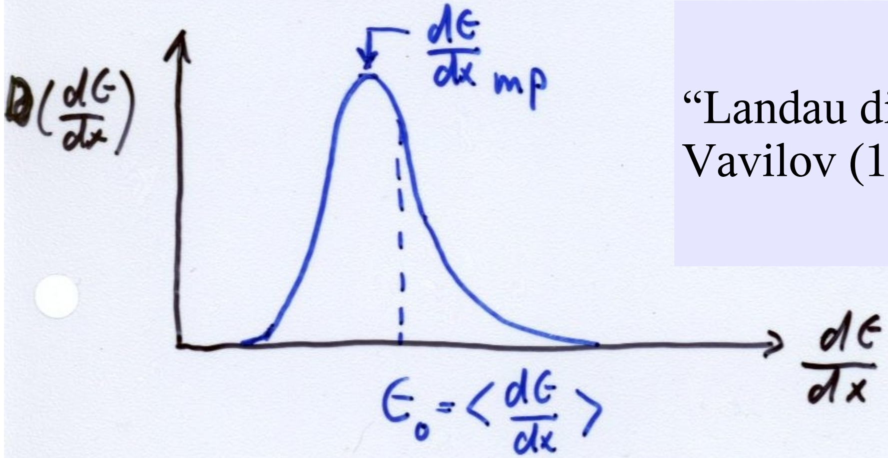

“Landau distribution” for thin absorber
Vavilov (1957): correction for thicker abs.

Approximation: $D\left(\frac{dE}{dx}\right) = \frac{1}{\sqrt{2\pi}} \exp\left(-\frac{1}{2}\left(\underbrace{\frac{\frac{dE}{dx} - \frac{dE}{dx}_{mp}}{\xi}}_{\lambda} + e^{-\lambda}\right)\right)$

ξ material constant

more precise: Allison & Cobb (using measurements and numerical solution) Ann. Rev. Nuclear Sci. 30 (1980) 253

Energy loss distribution normalized to thickness x

with increasing thickness:

- most probable $\Delta E/\Delta x$ shifts to large values
- relative width shrinks

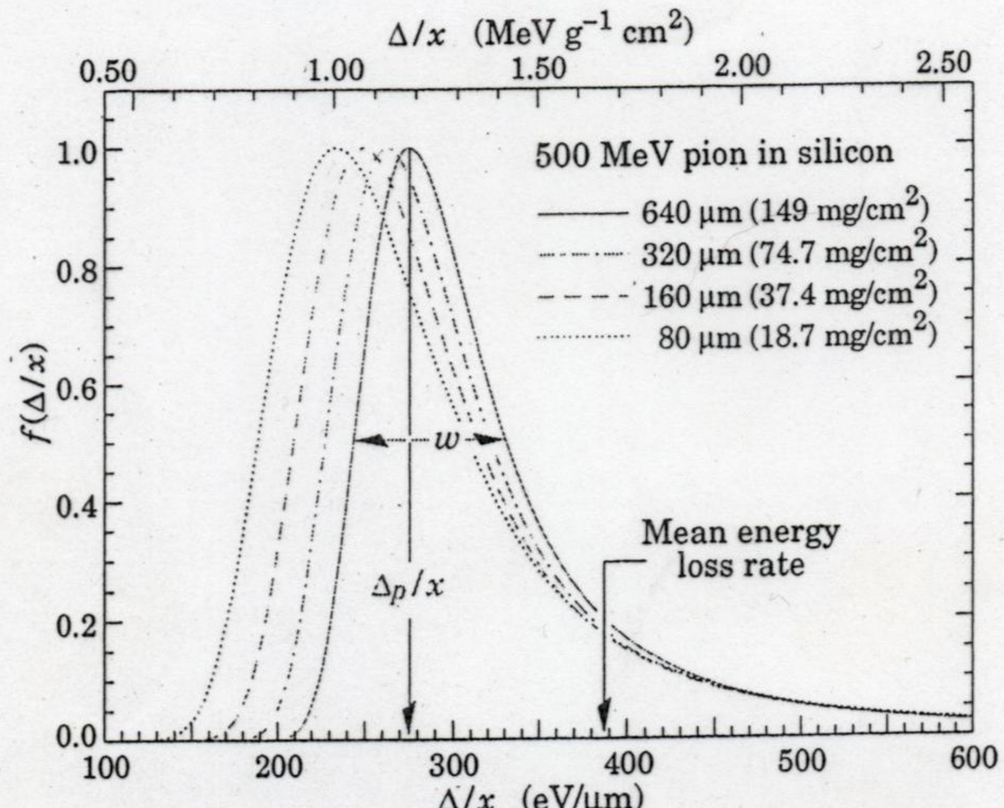

Figure 26.6: Straggling functions in silicon for 500 MeV pions, normalized to unity at the most probable value Δ_p/x. The width w is the full width at half maximum.

- asymmetry of distribution decreases

2.1.5 Multiple (Coulomb) scattering

in deriving energy loss by ionisation we had considered transv. momentum transfer to electron

$$\Delta p_\perp \approx \frac{2ze^2}{bv}$$

corresponding momentum transfer to primary particle. But here most visible deflection by target nuclei due to factor Z

$$\Theta \approx \frac{\Delta p_t}{p_\parallel} \approx \frac{\Delta p_t}{p} = \frac{2Zze^2}{b}\,\frac{1}{p\cdot v}$$

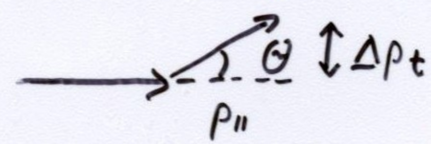

after k collisions

$$\langle \Theta_k^2 \rangle = \sum_{m=1}^{k} \Theta_m^2 = k \langle \Theta^2 \rangle$$

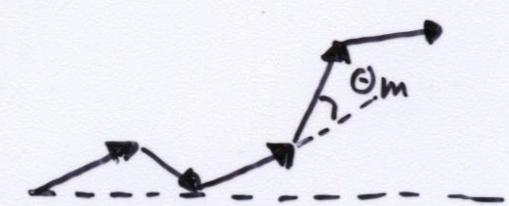

for very thin absorber: single collision, Rutherford scattering $d\sigma/d\omega \propto \sin^{-4}(\theta/2)$
for a few collisions: difficult
for many collisions (>20) statistical treatment Moliere theory (G.Z.Moliere 1947,1948)
averaging over many collisions and integration over b

averaging over many collisions and integrating over b, the mean deflection angle in a plane is

$$\boxed{\sqrt{\langle \Theta^2(x) \rangle} = \frac{13.6\ \text{MeV}}{\beta \cdot pc} \cdot z \sqrt{\frac{x}{X_0}} \left(1 + 0.038 \ln \frac{x}{X_0}\right)}$$

X_0 = material constant = “radiation length”

in 3 D : $\Theta_{rms} = \sqrt{2}\ \Theta_{rms}^{plane}$ d.h. $13.6 \rightarrow 19.2$

at small momenta this multiple scattering effect limits the momentum and vertex resolution

2.2. Interactions of photons with matter

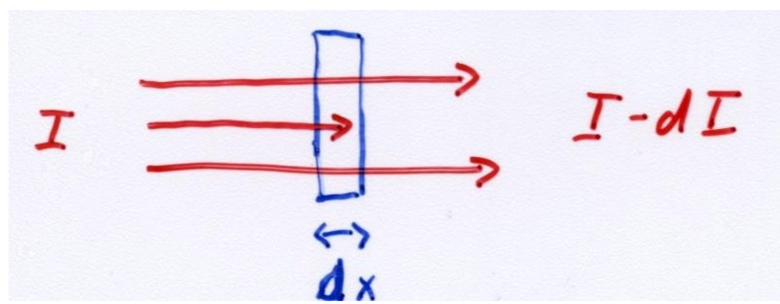

characteristic for photons: in a single interaction a photon can be removed out of beam with intensity I

$dI = - I\ \mu\ dx$ $\mu(E,Z,\rho) \rightarrow$ absorption coefficient

Lambert-Beer law of attenuation: $\boxed{I = I_0 \exp(-\mu x)}$

- mean free path of photon in matter: $\lambda = 1/n\sigma = 1/\mu$

to become independent of state (gaseous, liquid) and reduce variations → introduce mass absorption coefficient $\tau = \mu/\rho = N_A \sigma / A$

example: E_γ=100 keV, in iron Z=26, λ=15 g/cm^2 or 2 cm

3 processes, importance changing with photon energy

- photo effect
- Compton scattering
- pair production

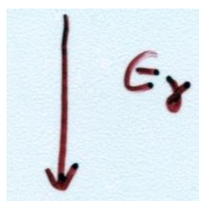

also present, but for energy loss not as important

- Rayleigh scattering (coherent on entire atom) $\gamma + e_b \rightarrow \gamma + e_b$
- photo nuclear absorption $\gamma + \text{nucleus} \rightarrow \text{p o. n} + \text{nucleus}$
- pair production on electron

2.2.1 Photo Effect

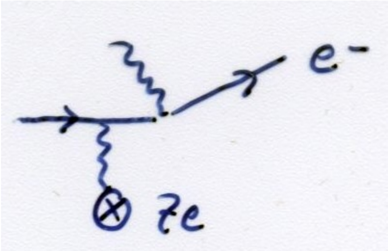

$\gamma + \text{atom} \rightarrow \text{atom}^+ + e^-$

$E_e = h\nu - I_b$

$h\nu$: γ–energy

I_b: binding energy of electron; K,L,M absorption edges

since binding energy strongly Z-dependent, strong Z-dependence of cross section

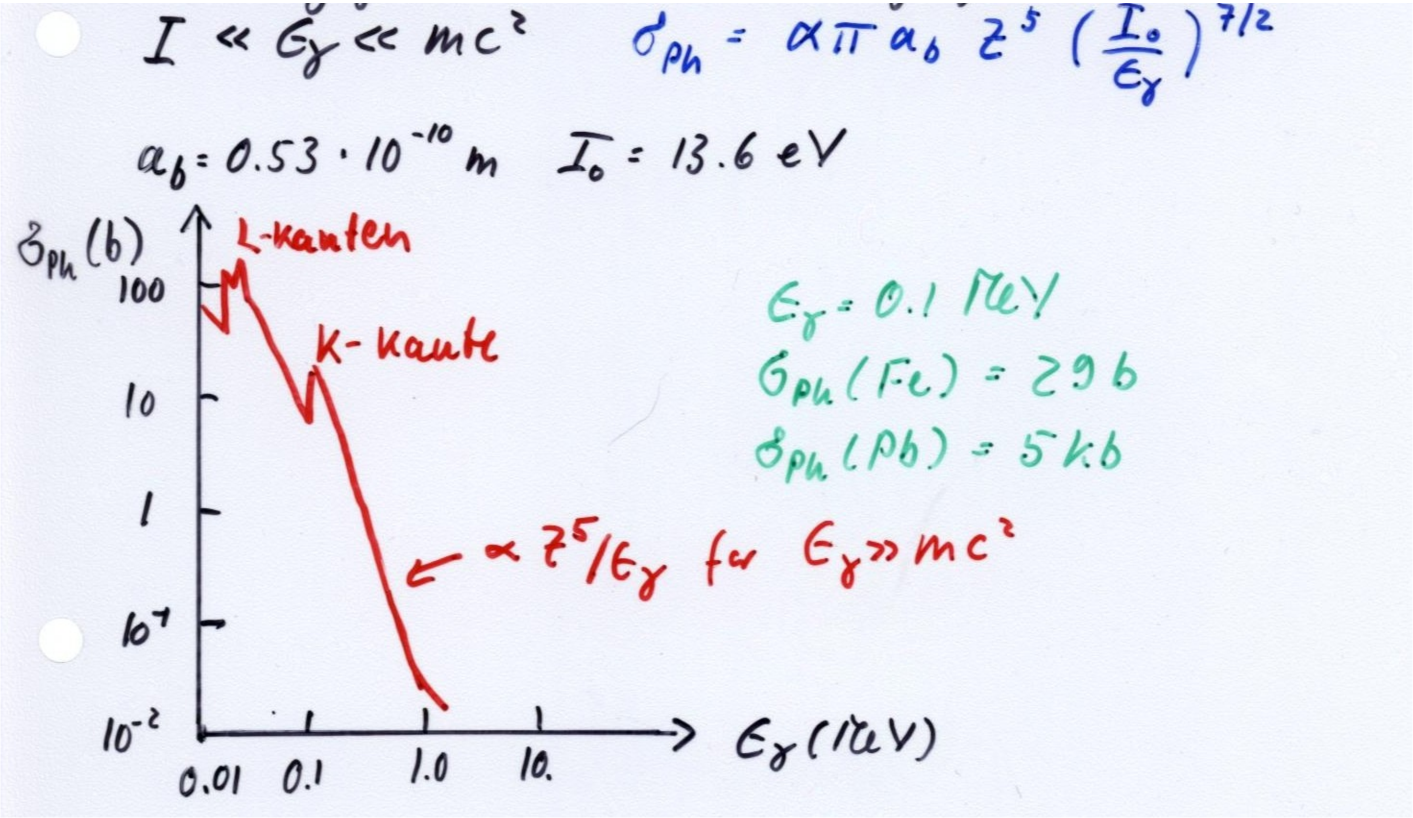

The excited atom emits either

X-rays $\quad atom_K^{+*} \rightarrow atom_{LM}^{+*} + \gamma$

or Auger electrons $\quad \rightarrow atom_{LM}^{++*} + e^-$

Auger electrons have small energy that is deposited locally
X-ray $\rightarrow$ photo effect again, range may be significant
this "fluorescence yield" increases with Z

2.2.2 Compton scattering

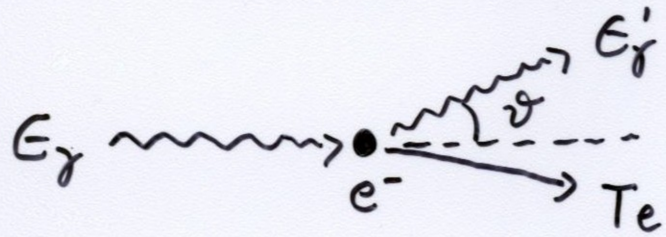

$$\frac{1}{E'_\gamma} - \frac{1}{E_\gamma} = \frac{1}{m_e c^2}(1-\cos\vartheta)$$
$$\leq \frac{2}{m_e c^2}$$

recoil of electron

$$T_e = \frac{\frac{E_\gamma}{m_e c^2}(1-\cos\vartheta)}{\frac{E_\gamma}{m_e c^2}(1-\cos\vartheta)+1} E_\gamma \qquad \left(\frac{T_e}{E_\gamma}\right)_{max} = \frac{E_\gamma}{m_e c^2}\,\frac{2}{1+2E_\gamma/m_e c^2}$$

$$\text{und} \quad \Delta E = E_\gamma - T_{e\,max} = \frac{E_\gamma}{1+\frac{2E_\gamma}{m_e c^2}} \longrightarrow \frac{m_e c^2}{2} \quad \text{für } E_\gamma \gg m_e c^2$$

Compton edge: in case scattered photon is not absorbed in detector, a minimal amount of energy is missing from the “full energy peak” (asymptotically half electron rest mass)

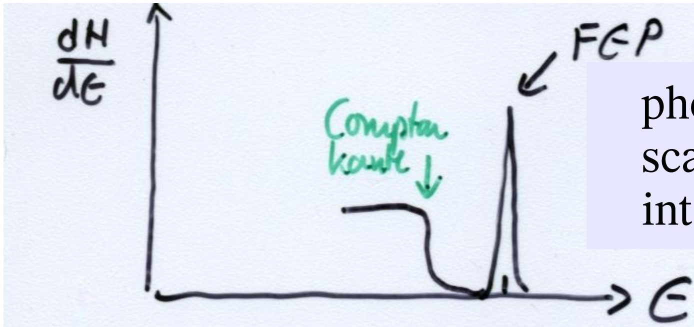

photo effect and Compton effect in case
scattered photon is absorbed
intensity depends on detector volume

- Cross section: calculation in QED

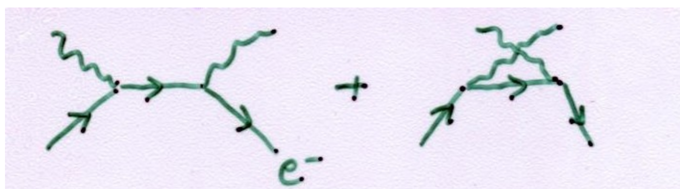

Klein - Nishima

- order of magnitude given by Thompson cross section

$$\sigma_{Th} = \frac{8\pi}{3} r_e^2 = 0.66\ b \qquad \gamma + e^- \rightarrow \gamma + e^- \qquad E_\gamma \rightarrow 0$$

- Compton: $E_\gamma \ll m_e c^2 \qquad \sigma_C = \sigma_{Th}\left(1 - \frac{2E_\gamma}{m_e c^2}\right)$

$E_\gamma \gg m_e c^2 \qquad \sigma_C = \frac{3}{8}\sigma_{Th}\frac{m_e c^2}{E_\gamma}\left(\ln\left(\frac{2E_\gamma}{m_e c^2}\right) + \frac{1}{2}\right)$

- angular distribution from QED – Klein-Nishina formula

$$\frac{d\sigma_c}{d\Omega} = \frac{r_e^2}{2} \cdot \frac{1}{\left(1+\varepsilon(1-\cos\vartheta)\right)^2}\left[1+\cos\vartheta + \frac{\varepsilon^2(1-\cos\vartheta)^2}{1+\varepsilon(1-\cos\vartheta)}\right]$$

$$\varepsilon = E_\gamma / m_e c^2$$

angular distribution of scattered photon

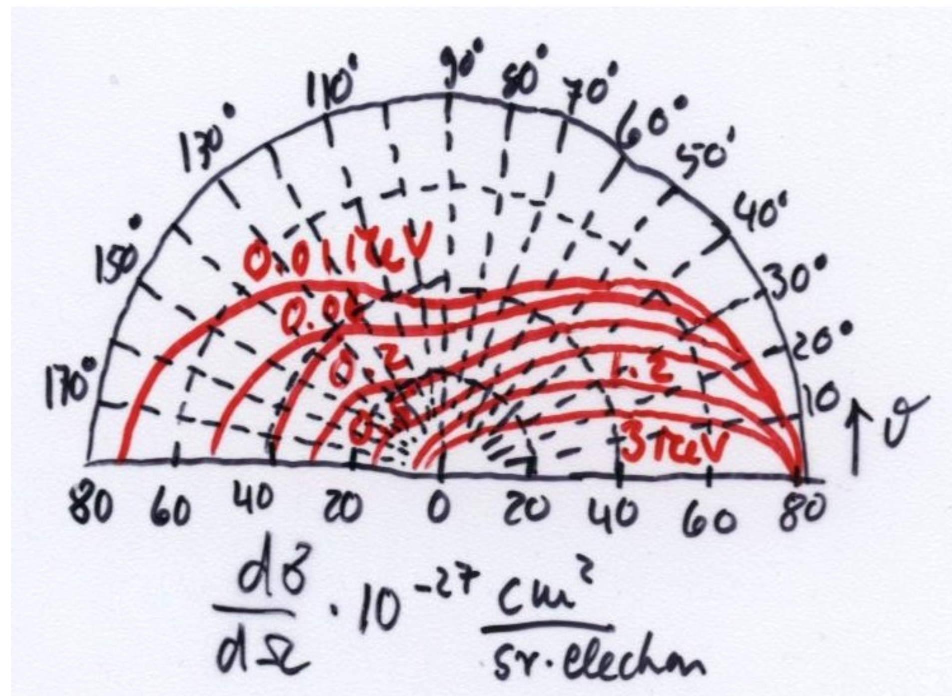

for high γ-energies forward peaked

- Spectrum of recoil electrons from Klein-Nishina formula after angular integration:

$$\frac{d\sigma_c}{dT_e} = \frac{\pi r_e^2}{m_e c^2 \varepsilon^2}\left[2 + \frac{s^2}{\varepsilon^2(1-s)^2} + \frac{s}{1-s}\left(s - \frac{2}{\varepsilon}\right)\right]$$

$\varepsilon = E_\gamma / m_e c^2 \qquad s = T_e / E_\gamma$

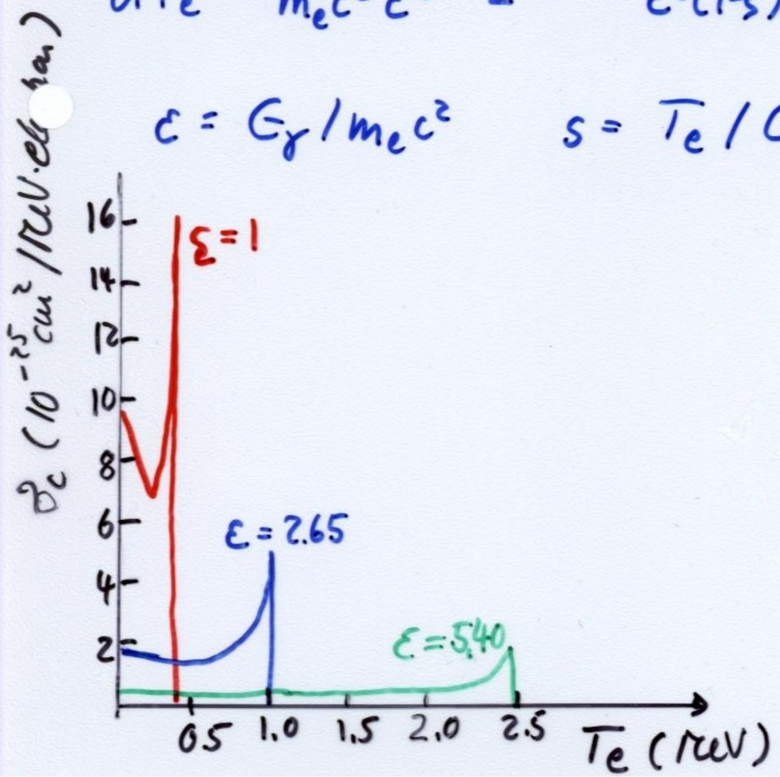

$$T^e_{max} = E_\gamma(1 - m_e/2E_\gamma)$$

- mass absorption coefficient

$$\mu_c = \frac{N_A \cdot \rho}{A} Z \sigma_c \sim \frac{Z \ln E_\gamma}{E_\gamma}$$

2.2.3 Pair production (Bethe-Heitler process)

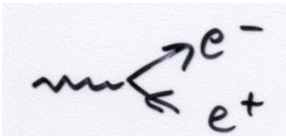

not possible in free space but in Coulomb field of atomic nucleus, to absorb recoil

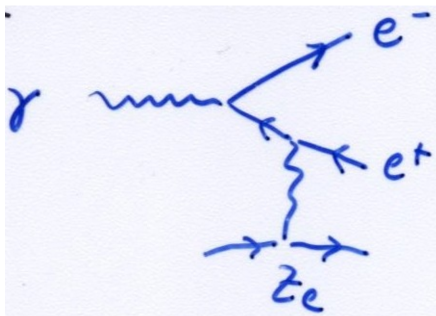

energy threshold

$$E_\gamma \gtrsim 2 m_e c^2 + 2\frac{m_e^2 c^4}{m_K c^2}$$

• Cross section: for low energies impact paramter small, photon sees naked nucleus with increasing E_γ impact parameter b is growing up to $b \geq a_{Atom}$,complete screening -> saturation of cross section

$$\sigma_p = 4 Z^2 \alpha r_e^2 \left(\frac{7}{9} \ln \frac{183}{Z^{1/3}} - \frac{1}{54} \right)$$

for $E_\gamma \gg m_e c^2$

$$\boxed{\sigma_p \simeq \frac{7}{9}\underbrace{\left(4 \alpha r_e^2 Z^2 \ln \frac{183}{Z^{1/3}}\right)}_{A/N_A X_0}}$$

$A/N_A X_0 \leftarrow$ radiation length $\left(\frac{g}{cm^2}\right)$

$\rho X_0 \Rightarrow$ length (cm)

$$\mu_p = \frac{N_A}{A}\sigma_p \simeq \frac{7}{9}\frac{1}{X_0}$$

definition of radiation length X_0: in terms of energy loss of electron by bremsstrahlung below examples:

	ϱ (g/cm^3)	X_0 (cm)
fl. H_2	0.071	865
C	2.27	18.8
Fe	7.87	1.76
Pb	11.35	0.56
Luft	$1.2 \cdot 10^{-3}$	30 420

the angular distribution of produced electrons is narrow in forward cone with opening angle of $\theta \approx \mathrm{m_e}/\mathrm{E}_\gamma$

fractional electron (or positron) energy x:

cross section necessarily symmetric between x and (1-x)

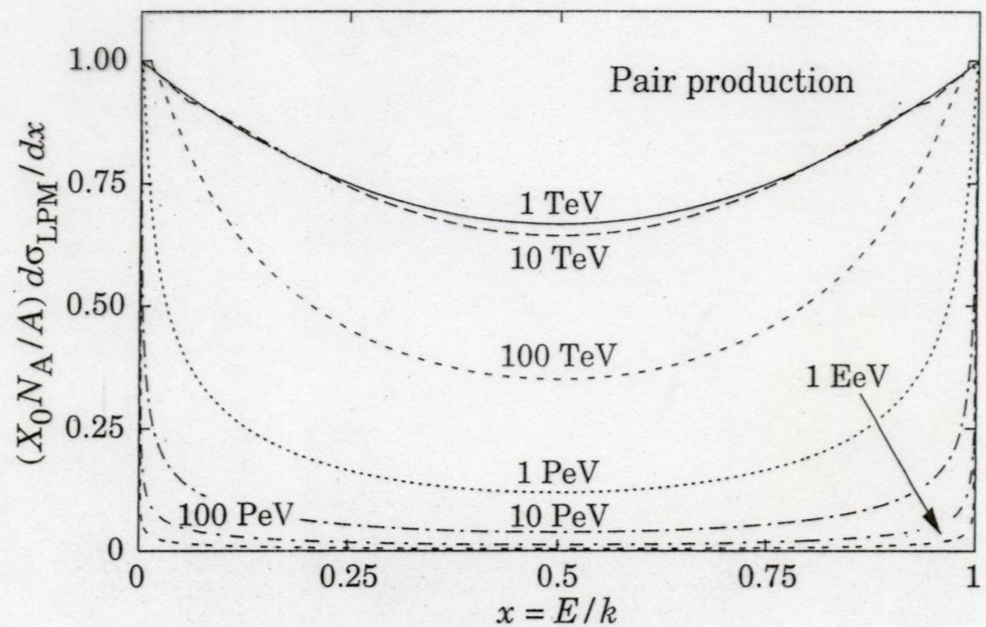

Figure 26.14: The normalized pair production cross section $d\sigma_{LPM}/dy$, versus fractional electron energy $x = E/k$.

at ultrahigh energies new effect – **Landau Pomeranchuk Migdal effect:**
quantum mechanical interference between amplitudes from different scattering centers;
relevant scale **formation length** – length over wich highly relativistic electron and photon split apart; interference (generally) destructive -> reduced cross section
for a given, very high photon energy: if electron (or positron) energy are above some value given by $E(k-E) > k\, E_{LPM}$ -> effect is visible, cross section reduced

$E_{LPM} = 7.7$ TeV/cm X_0 e.g. for Pb $E_{LPM} = 4.3$ TeV

take k = 100 TeV, suppression for E>4.5 TeV or x=0.045 (see also bremsstrahlung below)

2.2.4. Total absorption coefficient

$$\sigma_{tot} = \sigma_{ph} + \sigma_C + \sigma_P$$

$$\mu = \mu_{ph} + \mu_C + \mu_P \qquad \mu_i = n\sigma_i = \frac{N_A \varrho}{A}\sigma_i$$

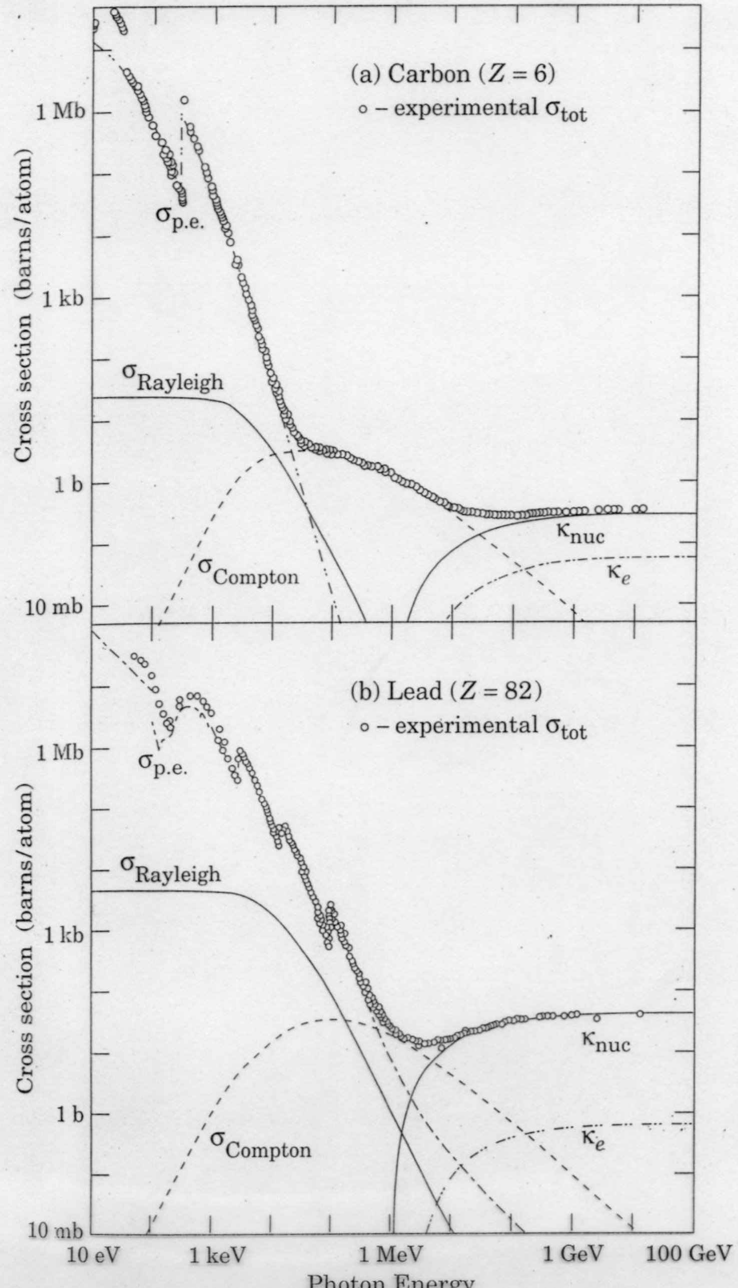

Figure 26.13: Photon total cross sections as a function of energy in carbon and lead, showing the contributions of different

photon mass attentuation length $\lambda=1/(\mu/\rho)$ mean free path

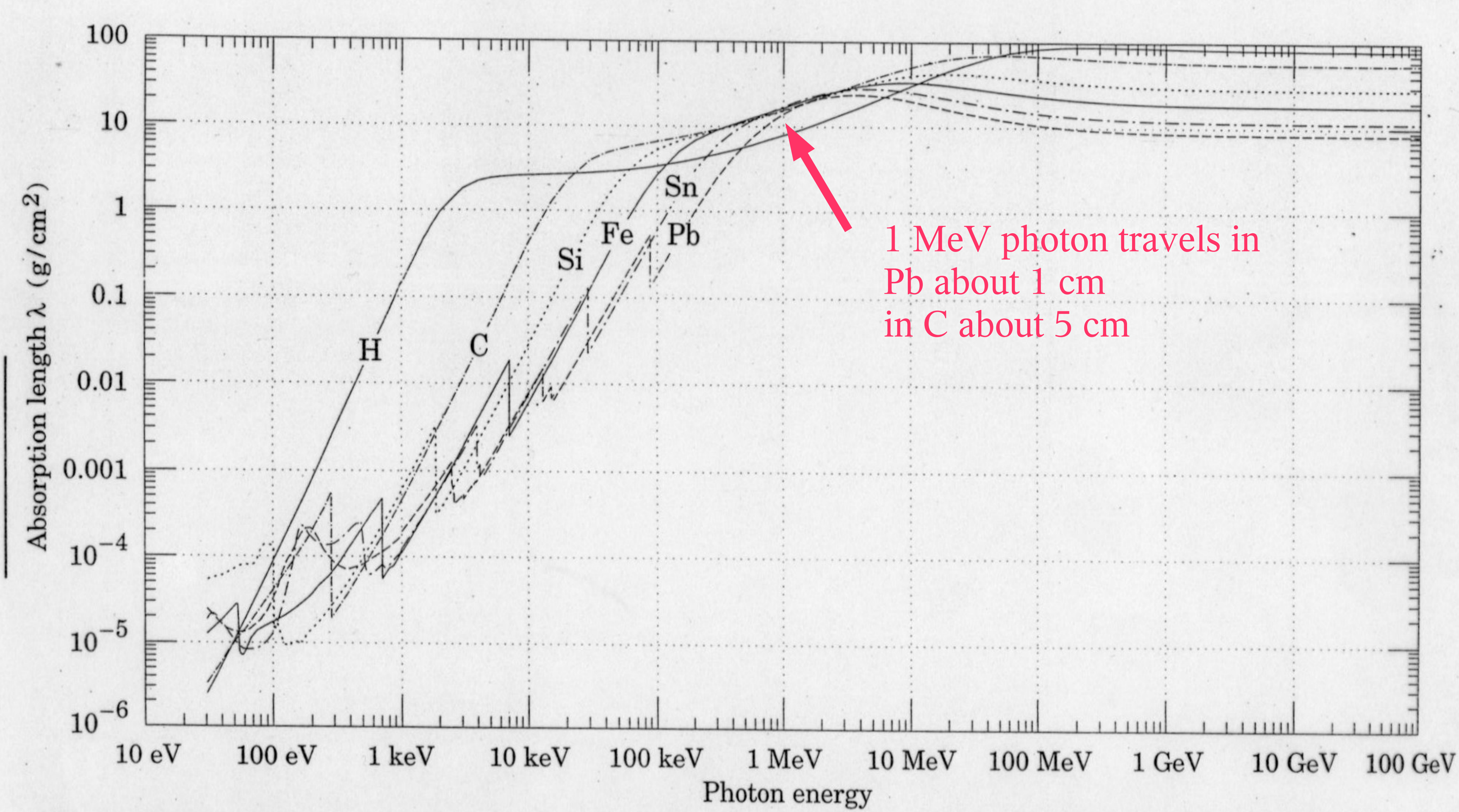

Fig. 26.15: The photon mass attenuation length (or mean free path) $\lambda = 1/(\mu/\rho)$ for various elemental absorbers as a function of photon energy. The mass attenuation coefficient is μ/ρ, where ρ is the density. The intensity I remaining after traversal of thickness t (in mass/unit area) is given by $I = I_0 \exp(-t/\lambda)$. The accuracy is a few percent. For a chemical compound or mixture, $\boxed{1/\lambda_{\text{eff}} \approx \sum_{\text{elements}} w_Z/\lambda_Z,}$ where w_Z is the proportion by weight of the element with atomic number Z. The processes responsible for attenuation are given in not Fig. 26.9. Since coherent processes are included, not all these processes result in energy deposition. The data for 30 eV $< E <$ 1 keV are obtained from `http://www-cxro.lbl.gov/optical_constants` (courtesy of Eric M. Gullikson, LBNL). The data for 1 keV $< E <$ 100 GeV are from `http://physics.nist.gov/PhysRefData`, through the courtesy of John H. Hubbell (NIST).

with increasing photon energy pair creation becomes dominant
for Pb beyond 4 MeV
for H beyond 70 MeV

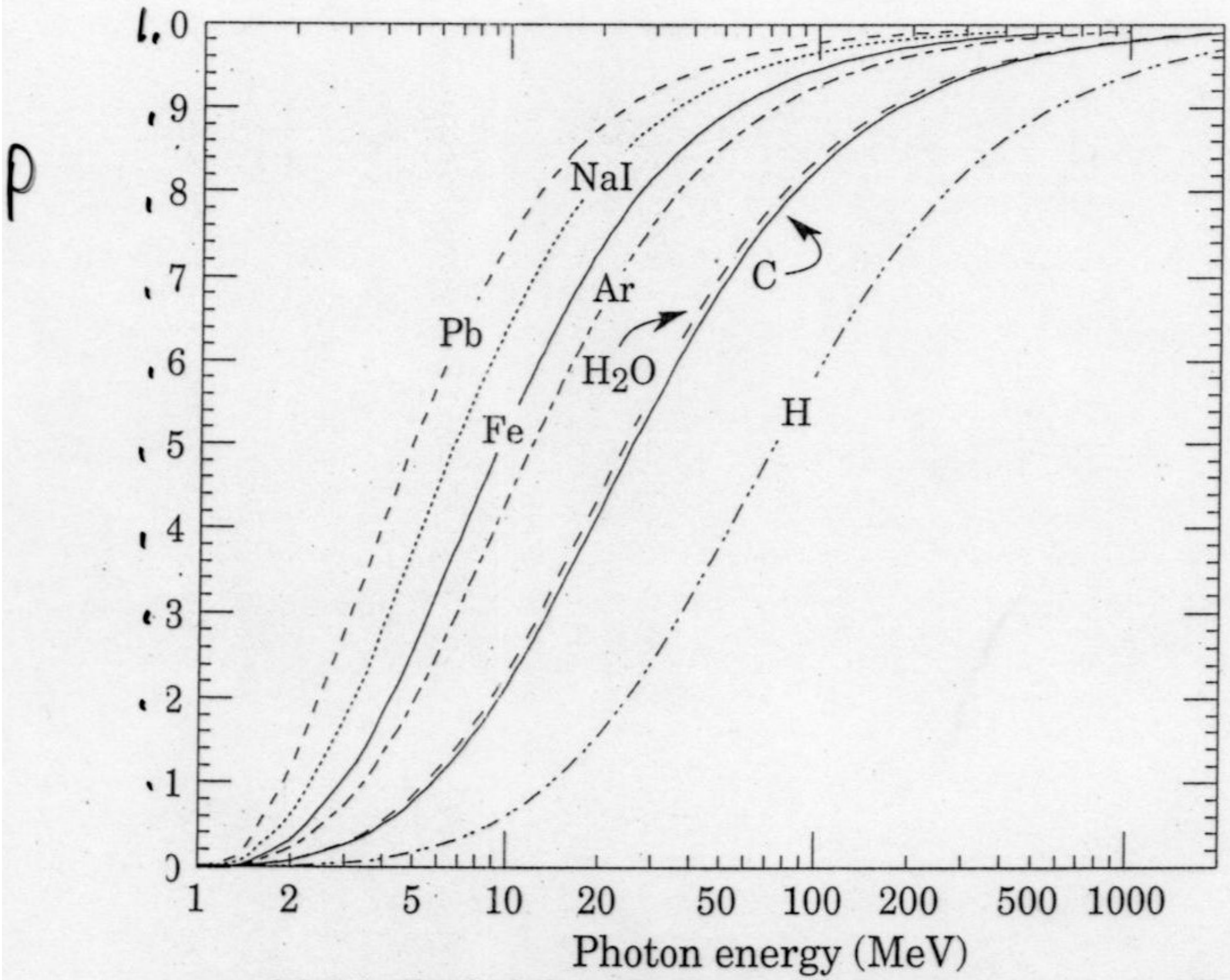

gure 26.16: Probability P that a photon interaction will ult in conversion to an e^+e^- pair. Except for a few-percent ıtribution from photonuclear absorption around 10 or 20 :V, essentially all other interactions in this energy range result Compton scattering off an atomic electron. For a photon enuation length λ (Fig. 26.15), the probability that a given ɔton will produce an electron pair (without first Compton ttering) in thickness t of absorber is $P[1 - \exp(-t/\lambda)]$.

2.3 Electrons

2.3.1 Energy loss by ionisation

modification of Bethe-Bloch equation

m_e small $\rightarrow$ deflection important

identical particles $\rightarrow$ $W_{max} = T/2$

quantum mechanics: after scattering no way to distinguish between incident electron and electron from ionisation

for relativistic electrons

$$-\frac{dE}{dx} = 4\pi N_A r_e^2 m_e c^2 \frac{Z}{A} \frac{1}{\beta^2} \left[\ln \frac{\gamma m_e c^2 \beta \sqrt{\gamma - 1}}{\sqrt{2}\, I} + F(\gamma) \right]$$

considers kinematics of $e^- + e^-$ collision and screening

Positrons: for small energies energy loss a bit larger (annihilation); also: they are not identical particles

Remark: for same β the energy loss by ionisation for e^- and p within 10 % equal ionisation yield: (this part also valid for heavy particles as treated above)

Mean energy loss by ionisation and excitation can be transformed into mean number of electron-ion pairs produced along track of ionising particle
total ionisation = primary ionisation + secondary ionisation due to energetic primary electron

$$\boxed{n_t = n_p + n_s}$$

with mean energy W to produce an electron-ion pair

$$\boxed{n_t = \frac{\Delta E}{W}}$$

W > ionisation potential I_0 since

- also ionisation of inner shells
- excitation that may not lead to ionisation

$$n_t \approx (2-6)n_p$$

typische Werte

	I_0(eV)	W(eV)	n_p(cm^{-1})	n_t(cm^{-1})
H_2	15.4	37	5.2	9.2
N_2	15.5	35	10	56
O_2	12.2	31	22	73
Ne	21.6	36	12	39
Ar	15.8	26	29	94
Kr	14.0	24	22	192
Xe	12.1	22	44	307
CO_2	13.7	33	34	91
CH_4	13.1	28	16	53

in Gasen ≈ 30 eV

Unterschiede durch Dichte

Solid state detectors:

	W (eV)
Si	3.6
Ge	2.85

and additional factor 10^3 due to density
-> many more electron ion pairs!

important difference electron – heavy particle

heavy particle: track more or less straight
electron: can be scattered into large angles

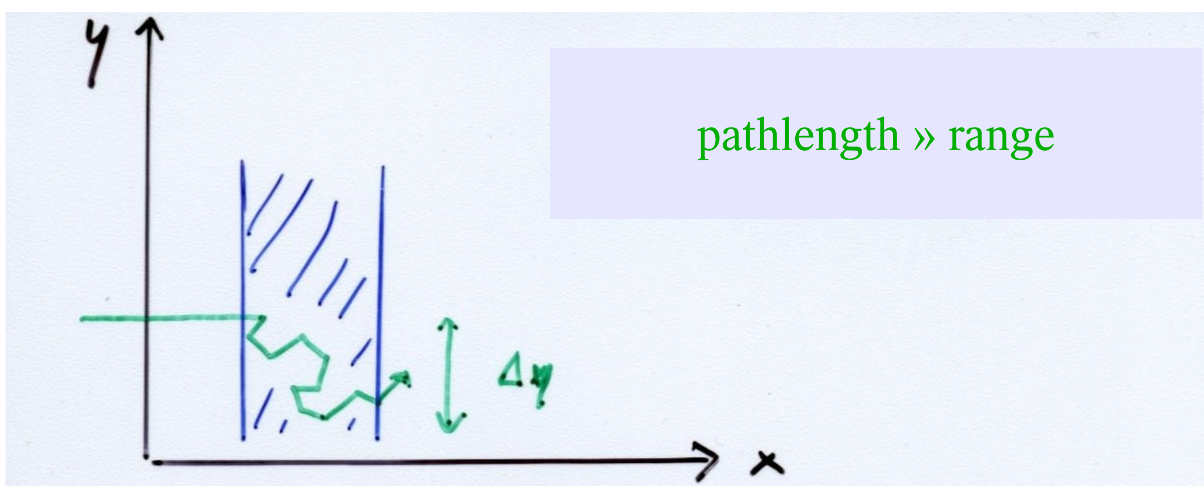

transverse deflection of an electron of energy $E = E_c$ (see below) after traversing distance X_0 (one radiation length)

$$\Delta y = R_M = \frac{21\ \text{MeV}}{E_c} X_0$$ "Molière radius"

	E_c (MeV)	R_M (cm)	X_0 (cm)
Pb	7.2	1.6	0.56
Szint.	80	9.1	42
NaI	12.5	4.4	2.6

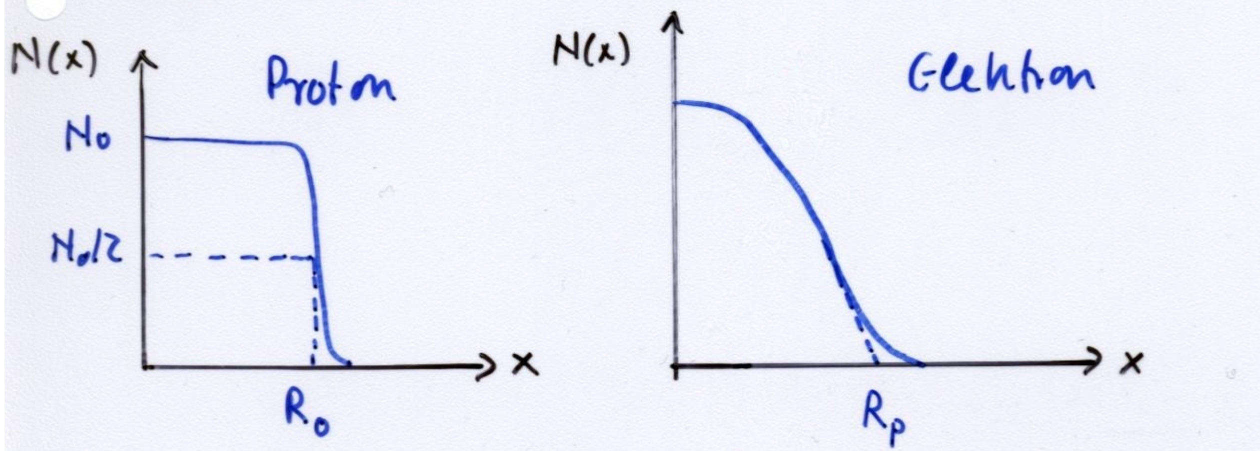

R_p: extrapolated range (rule of thumb)

$$R_p\left(\frac{g}{cm^2}\right) = 0.52\,T - 0.09 \quad \text{für} \quad T = 0.5 - 3\ \text{MeV}$$

2.3.2 Bremsstrahlung

QED process (Fermi 1924, Weizsäcker – Williams 1938)

lab system   rest system of electron

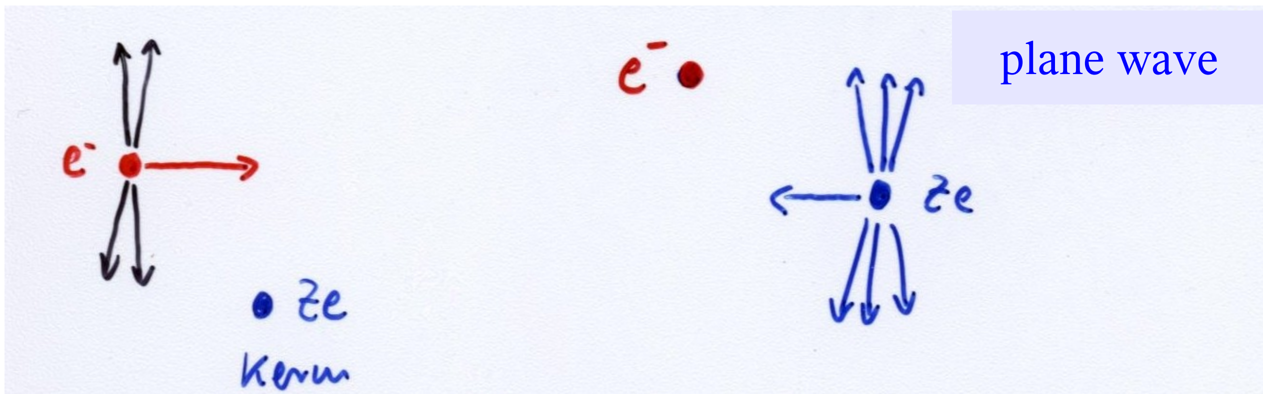

electron is hit by plane electromagnetic wave (for large v); E ⊥ B and both ⊥ v;
quanta are scattered by electrons and appear as real photons

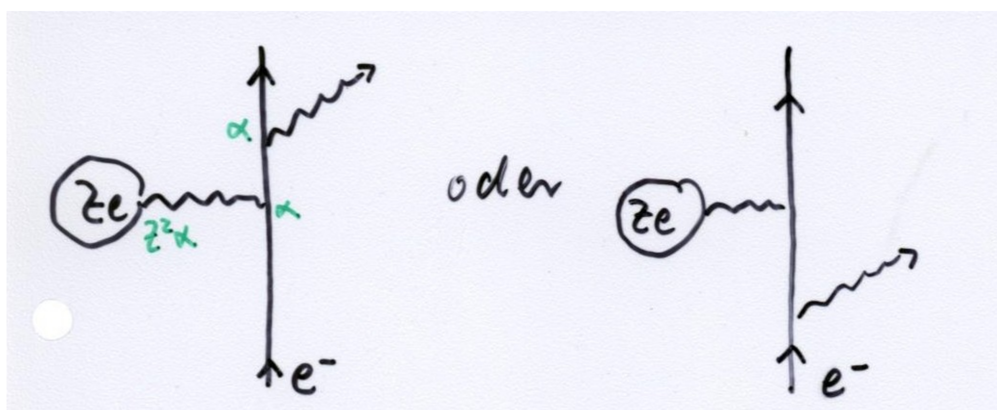

note: graph closely related to pair creation

in Coulomb field of nucleus electron is accelerated

amplitude of electromagnetic radiation $\propto$ acceleration $\propto 1/m_e c^2$

$$\boxed{\sigma_{brems} \propto \frac{Z^2 \alpha^3}{(m_e c^2)^2}}$$

spectrum of photons $\propto 1/k$

approximately $\frac{d\sigma}{dk} \simeq \frac{A}{X_0 N_A} \frac{1}{k} \left(\frac{4}{3} - \frac{4}{3} y + y^2 \right)$

with $y = k/E$
(corrections later)

→ normalized bremsstrahlung cross section
(in number of photons per radiation length)

$$\boxed{N_k = \frac{X_0 N_A}{A} k \frac{d\sigma}{dk} = \left(\frac{4}{3} - \frac{4}{3} y + y^2 \right)}$$

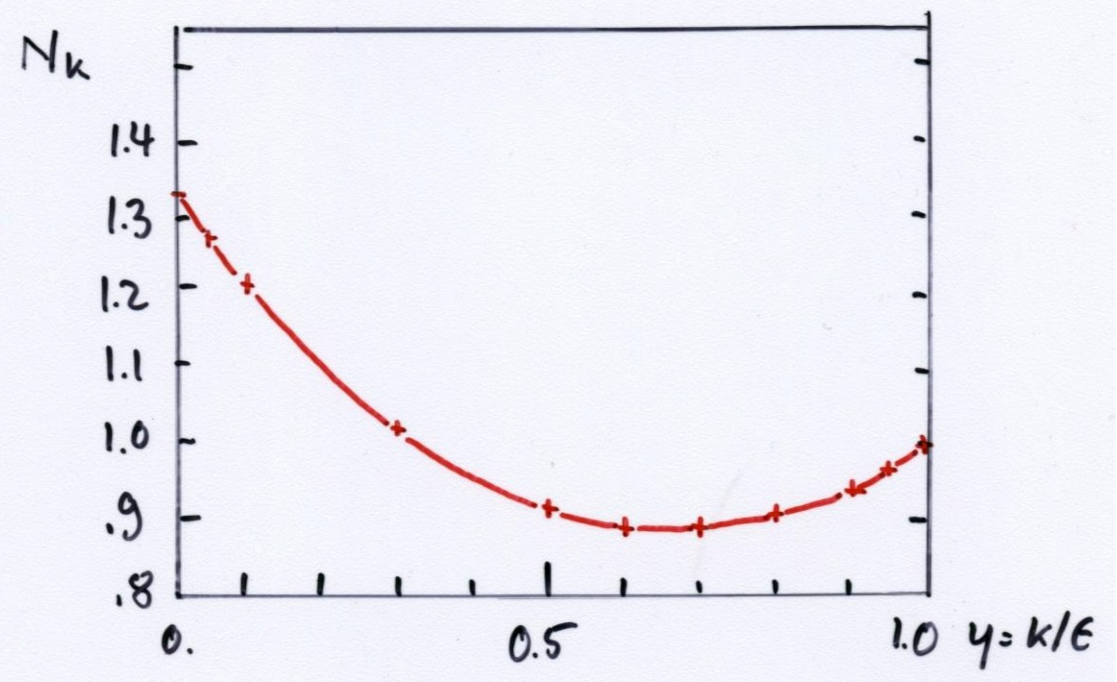

from this compute N_γ in interval dk and from this energy loss

$$\boxed{-\frac{dE}{dx} = 4\alpha N_A \frac{Z^2}{A} r_e^2 E \ln\frac{183}{Z^{1/3}}}$$

remark: $$r_e^2 = \frac{e^4}{(m_e c^2)^2} = \alpha^2\left(\frac{\hbar c}{m_e c^2}\right)^2 \longleftrightarrow -\frac{dE}{dx} \propto \frac{\alpha^3}{(m_e c^2)^2}$$

considering also interaction with electrons in atom

$$\boxed{-\frac{dE}{dx} = 4\alpha N_A \frac{Z(Z+1)}{A} r_e^2 E \ln\frac{287}{Z^{1/2}} = \frac{E}{X_0}}$$

So $E(x) = E_0 \exp(-x/X_0) \leftrightarrow X_0$ is distance over which energy decreases to 1/e of initial value

for mixtures:

$$\frac{1}{X_0} = \sum_i w_i / X_{0i}$$

weight fraction
of substance i

2.3.3. Total energy loss of electrons and positrons

critical energy:

$-\frac{dE}{dx}$ by ionisation grows as $\ln E$

$-\frac{dE}{dx}$ by bremsstrahlung grows $\propto E$

$\rightarrow$ existence of crossing point beyond which bremsstrahlung dominates

at $E = E_c$ = critical energy $\boxed{\left.\frac{dE}{dx}\right|_{ion} = \left.\frac{dE}{dx}\right|_{brems}}$

for electrons and Z > 13 $E_c = \frac{580}{Z}$ MeV

for muons $E_c = \frac{24}{Z}$ TeV

↑ negligible!

due to $\left(\frac{m_\mu}{m_e}\right)^2 = 4.3 \cdot 10^4$

critical energy for electrons in Cu:

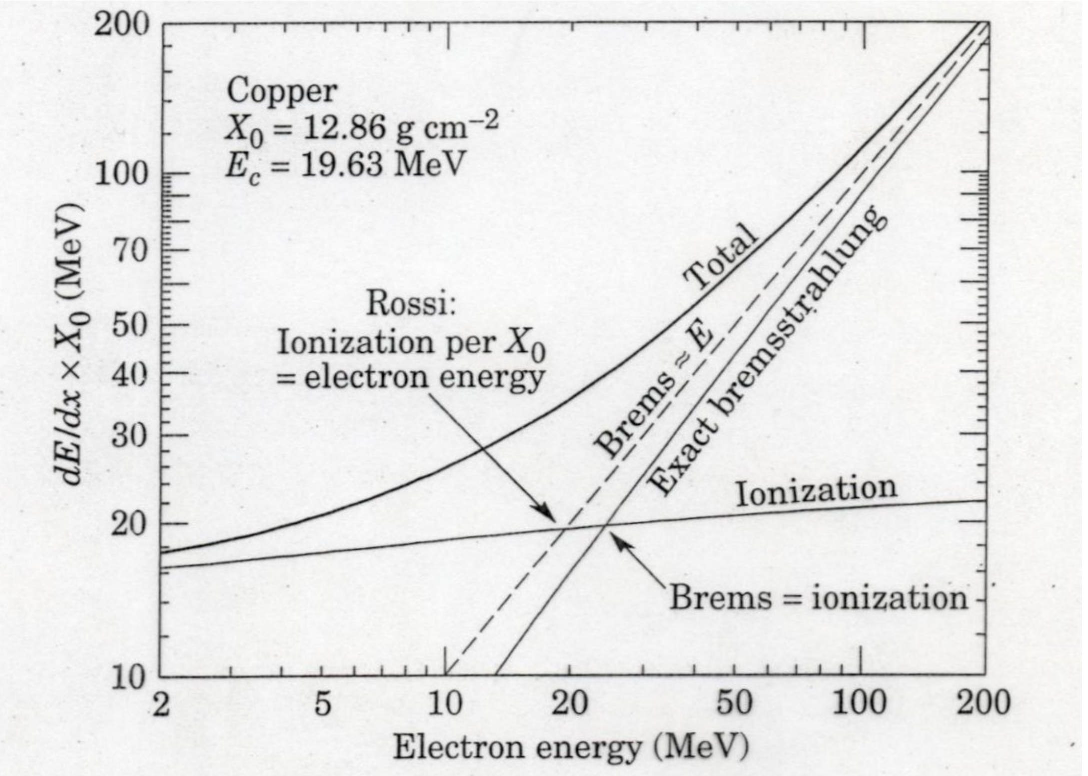

Figure 26.11: Two definitions of the critical energy E_c.

in the literature alternative definitions
i) energy at which loss rates of ionization and radiation equal
ii) energy at which ionization energy loss per rad. length is equal
to electron energy (equivalent in approx $dE/dx_{brems} = E/X_0$)
good for transverse em shower description

Total energy loss of electrons and positrons

at small energies also

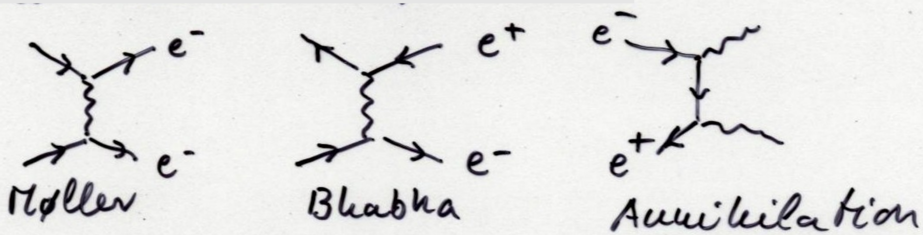

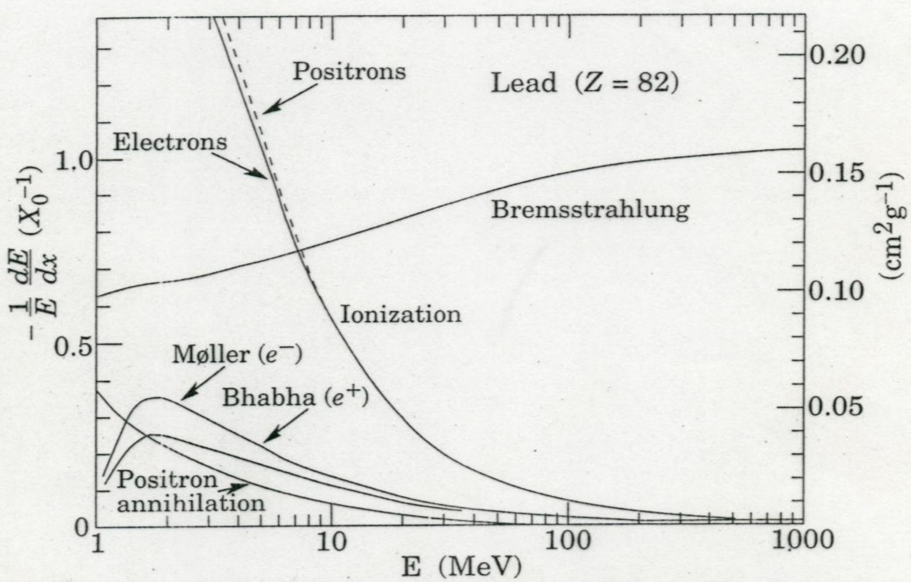

Figure 26.9: Fractional energy loss per radiation length in lead as a function of electron or positron energy. Electron (positron) scattering is considered as ionization when the energy loss per collision is below 0.255 MeV, and as Moller (Bhabha) scattering when it is above. Adapted from Fig. 3.2 from Messel and Crawford, *Electron-Photon Shower Distribution Function Tables for Lead, Copper, and Air Absorbers*, Pergamon Press, 1970. Messel and Crawford use $X_0(\mathrm{Pb}) = 5.82\ \mathrm{g/cm^2}$, but we have modified the figures to reflect the value given in the Table of Atomic and Nuclear Properties of Materials ($X_0(\mathrm{Pb}) = 6.37\ \mathrm{g/cm^2}$).

normalized bremsstrahlung cross section:

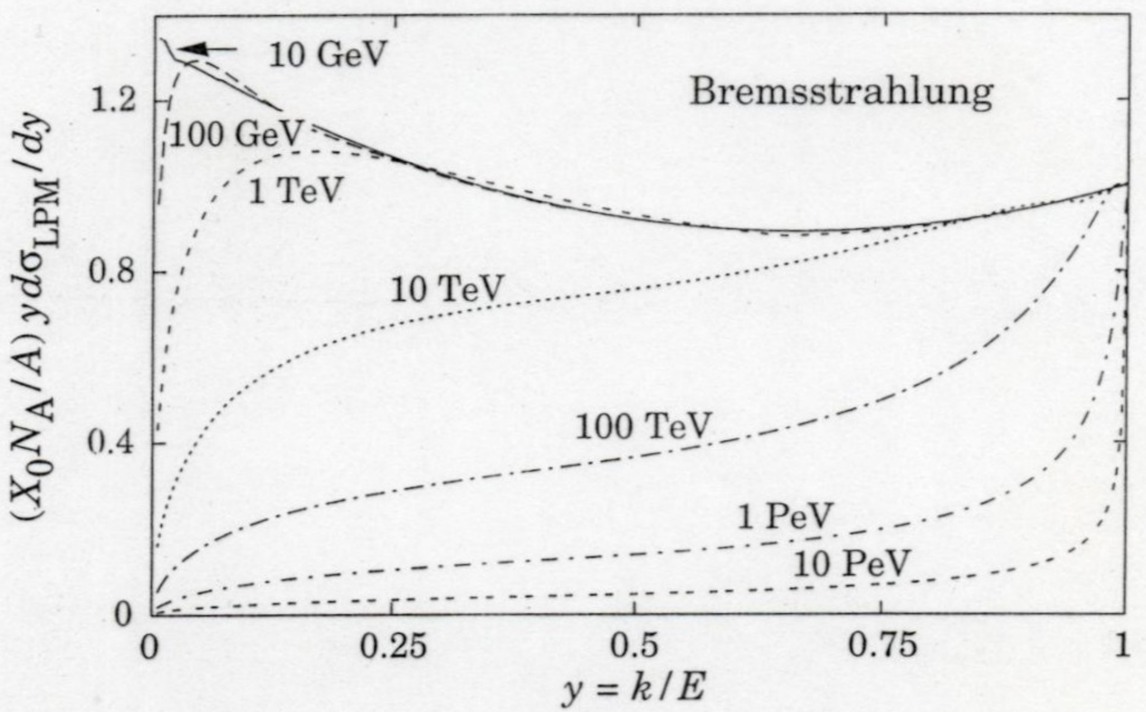

Figure 26.10: The normalized bremsstrahlung cross section $k\, d\sigma_{LPM}/dk$ in lead versus the fractional photon energy $y = k/E$. The vertical axis has units of photons per radiation length.

for small photon energies: again LPM effect important because successive radiations interfere radiation spread over formation length and if distance between successive radiations comparable to formation length -> destructive interference

for Pb and electron of 10 GeV suppression for $k<23$ MeV
100 GeV " $k<2.3$ GeV

quantum mechanical suppression of bremsstrahlung: important for very high energies
e.g. air showers of cosmic ray interactions

• in bremsstrahlung process nucleus absorbs longitudinal momentum

$$c|\vec{q}_\parallel| \simeq |\vec{p}_e| - |\vec{p}_e^{\,\prime}| - |\vec{p}_\gamma| \simeq \frac{E_\gamma}{2\gamma^2}$$

• corresponding to uncertainty principle momentum transferred over finite length scale (formation length)

$$L_F = \frac{\hbar c}{q_\parallel c} = \frac{2\gamma^2 \hbar c}{E_\gamma}$$

z.B. $E = 25\ \text{GeV}$ $E_\gamma = 100\ \text{MeV}$ $q_\parallel = 20\ \frac{\text{meV}}{c} \rightarrow L_F = 10\ \mu\text{m}$

semi-classical: photon emission and exchange of photon w. nucleus take place over length L_F
but only if electron and photon remain coherent over this length. Destruction of coherence via

a) Landau-Pomeranchuk-Migdal effect
decoherence by multiple scattering when $\sqrt{\vartheta^2_{ms}} = \frac{21\ \text{MeV}}{E}\sqrt{\frac{L_F}{X_0}} \geq \vartheta_\gamma = \frac{m}{E} = \frac{1}{\gamma}$

for E = 25 GeV and Au target suppression ↓ for $E_\gamma \leq 10$ MeV

b) dielectric effect
phaseshift of photons by dielectric constant; strong suppression for
$E_\gamma \leq \gamma\hbar\omega_p$ or $E_\gamma/E \leq 10^{-4}$

c) at large y screening may be incomplete

2.4. Cherenkov radiation

particle of mass M and velocity $\beta = v/c$ propagates through medium with real part of dielectic constant

$$\boxed{\varepsilon_1 = n^2 = \frac{c^2}{c_m^2}}$$

in case $\boxed{\beta > \beta_{thr} = \frac{1}{n}}$ or $v > c_m$

real photons can be emitted

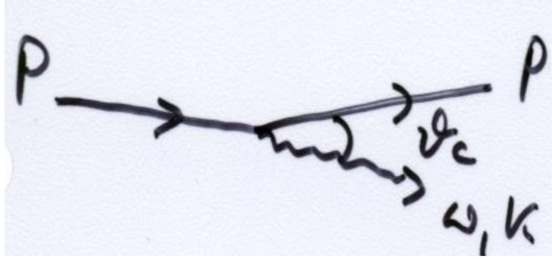

$$|p| \simeq |p'|$$

$$\omega \ll \gamma M c^2$$

under angle

$$\boxed{\cos\vartheta_c = \frac{\omega}{k \cdot v} = \frac{1}{n\beta}}$$

Cherenkov 1934

coherent wavefront

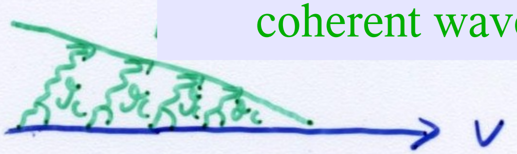

Applications

a) threshold detector: principle – if Cherenkov radiation observed $\rightarrow \beta > \beta_{thr}$
e.g. separation of π/K/p of given momentum *p*

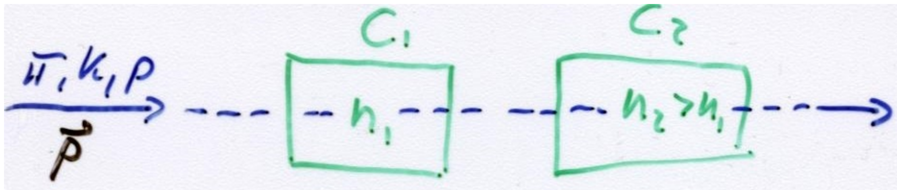

choose	n_2	such that	$\beta_\pi, \beta_K > \frac{1}{n_2}$	$\beta_p < \frac{1}{n_2}$
	n_1		$\beta_\pi > \frac{1}{n_1}$	$\beta_K, \beta_p < \frac{1}{n_1}$

light in C_1 and C_2: $\leftrightarrow$ π
light in C_1 and not in C_2: K
no light in C_1 and C_2: p

b) measurement of θ_c in medium with known n $\rightarrow \beta$
(RICH, DIRC, DISC detectors)

Spectrum and number of radiated photons

over range in ω where $\varepsilon_1 > \frac{1}{\beta^2}$

$$\boxed{dN_\gamma \propto d\nu = d\lambda/\lambda^2}$$

blue dominated

for distance x and frequency interval dν: $N_\gamma = x \underbrace{\frac{\alpha}{\hbar c}}_{370/\mathrm{eV\cdot cm}} \int_{\omega_1}^{\omega_2} \underbrace{\left(1 - \frac{1}{\beta^2 n^2(\omega)}\right)}_{\sin^2\vartheta_c} \hbar\, d\omega$

for interval dν, where n(ω) varies not much (e.g. gases around visible wavelength)
300 nm < λ < 600 nm: $N_\gamma = 750 \sin^2\theta_c/\mathrm{cm}$

	$(n-1)$	$\beta_{thr}\gamma_{thr}$	ϑ_c^∞	$N_\gamma\,(\mathrm{cm}^{-1})$
H_2	$0.14\cdot10^{-3}$	59.8	0.96°	0.21
N_2	$0.3\cdot10^{-3}$	40.8	1.4°	0.45
Freon 13	$0.72\cdot10^{-3}$	26.3	2.2°	1.1
Wasser	0.33	1.13	41.2°	165
Plexiglas	0.49	0.91	47.8°	412

typical photon energy: $\cong 3$ eV

in water: $dE/dx_{\text{Cher}} = 0.5$ keV/cm $= 0.5$ keV/g/cm^2

comparison with ionisation: $dE/dx_{\text{ion}} \geq 2$ MeV/g/cm^2

→ energy loss by Cherenkov radiation negligible

→ emission of scintillation light by excited atoms can fake Cherenkov radiation !

measurement of β requires minimum number of detected photoelectrons

$$n_e = n_\gamma\,(\text{Cherenkov}) \cdot \varepsilon_{\text{lightcoll}} \cdot \eta$$

$\cong 80$ %   quantum yield $\cong 20$ %

example: require for reconstruction of ring in RICH $n_e \geq 4$ and efficiency should be 90 %

n_e follows Poisson distribution

for a given $\langle n_e \rangle$ $P(4) + P(5) + P(6) + \ldots \geq 0.9$

$$P_n = \frac{\langle n_e \rangle^n \exp - \langle n_e \rangle}{n!}$$ Poisson

$\langle n_e \rangle = 7$ $\sum_0^3 P_n = 7.9\,\%$ Efficient für $n \geq 4$: $92.1\,\%$

need about 45 Cherenkov photons → about 0.5 m freon

Asymptotic Cherenkov angle and number of photons as function of momentum

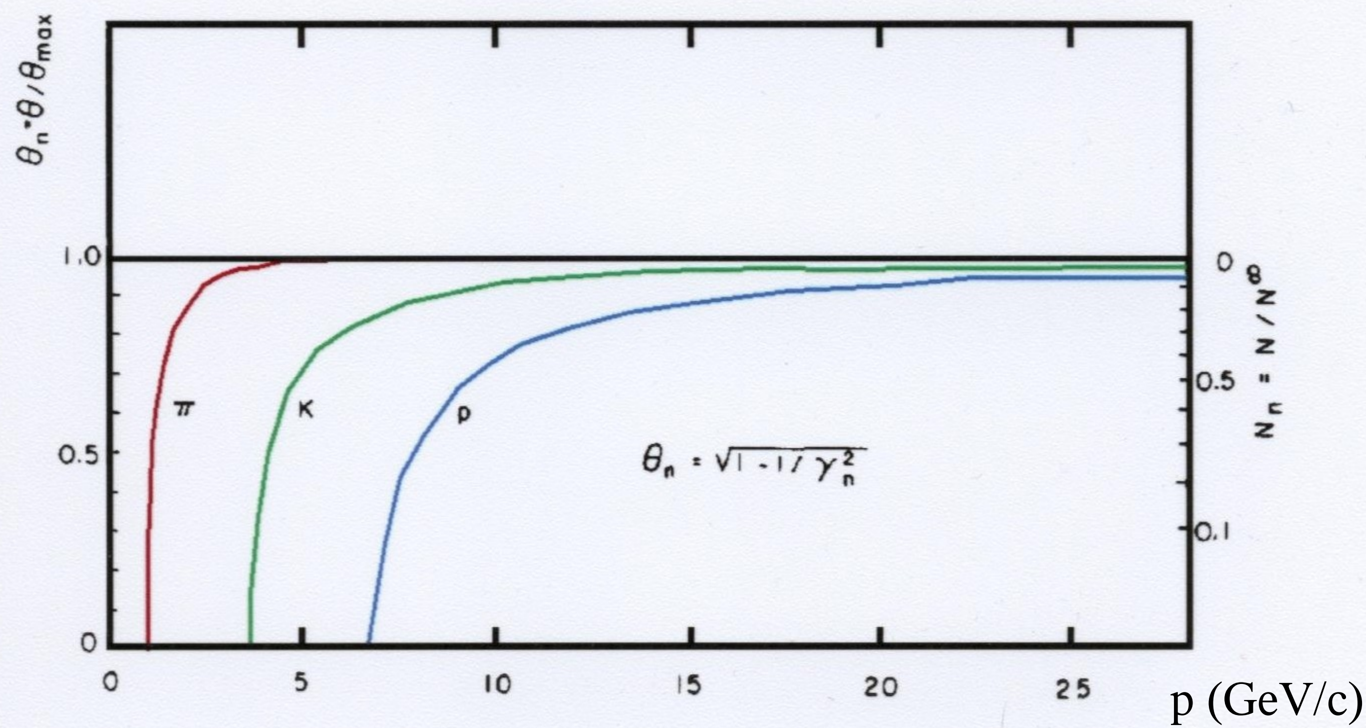

Number of photons grows with β and reaches asymptotic value for β → 1

$$\cos\vartheta_c^\infty = \frac{1}{n} \quad \text{och} \quad \vartheta_c^\infty = \text{acos}(1/n)$$

$$N_\gamma = x \cdot 370/\text{cm}\left(1 - \frac{1}{\beta^2 n^2}\right)$$

$$N_\gamma^\infty = x \cdot 370/\text{cm}\left(1 - \frac{1}{n^2}\right)$$

use of Cherenkov light for neutrino detection:
electron neutrinos: charged current events
all neutrinos: neutral current

leading to final state neutrino and energetic electron (typically E > 5 MeV to be above background from nat. radioactivity) detected by Cherenkov rad.

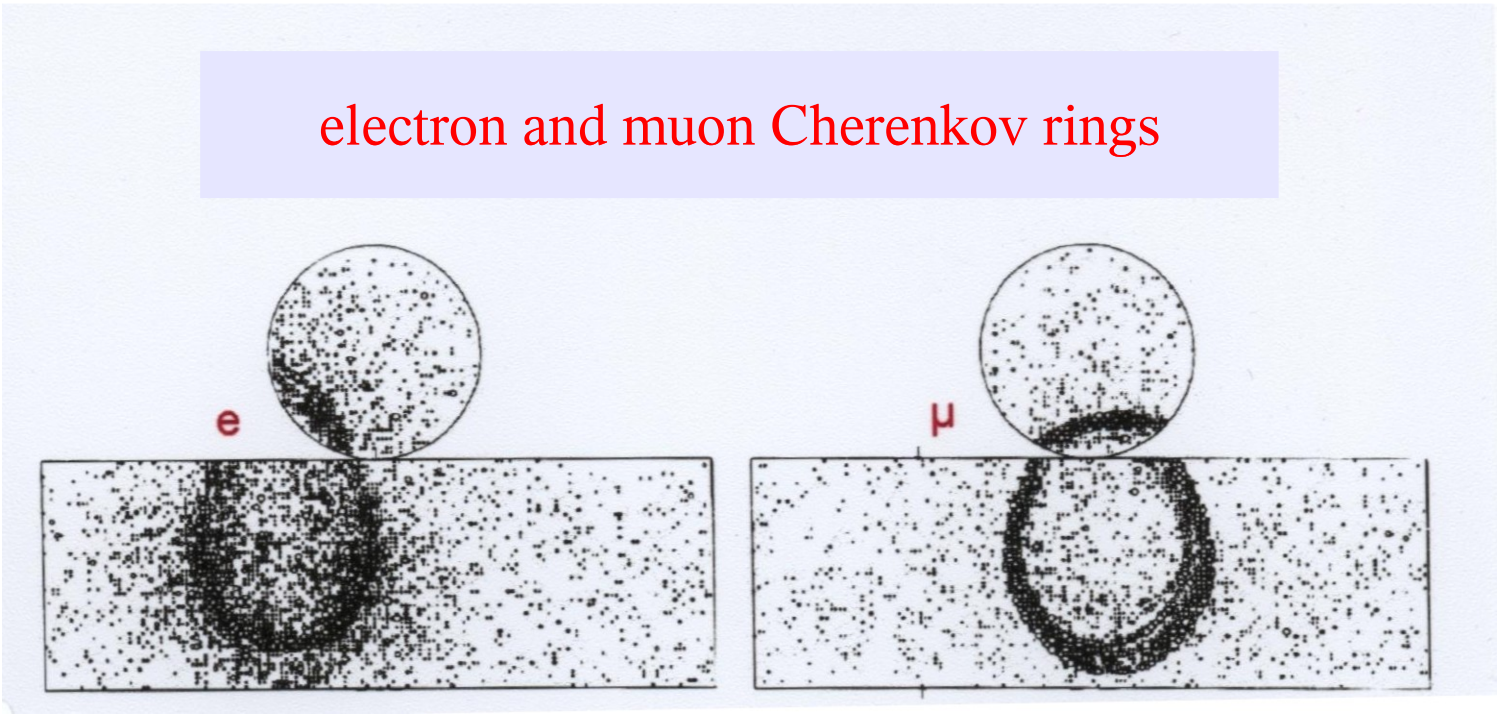

through multiple scattering electron ring becomes diffuse
can distinguish electron from muon
important for neutrino detectors (Superkamiokande, SNO)

2.5. Transition Radiation

A relativistic particle can emit a real photon when traversing boundary between 2 different dielectrics
predicted: Ginzburg and Frank 1946; confirmed in 1970 ies

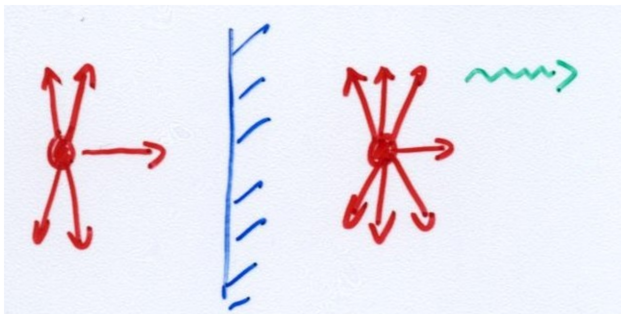

electric field needs to rearrange

simple model: electron moves in vacuum towards a conducting plate

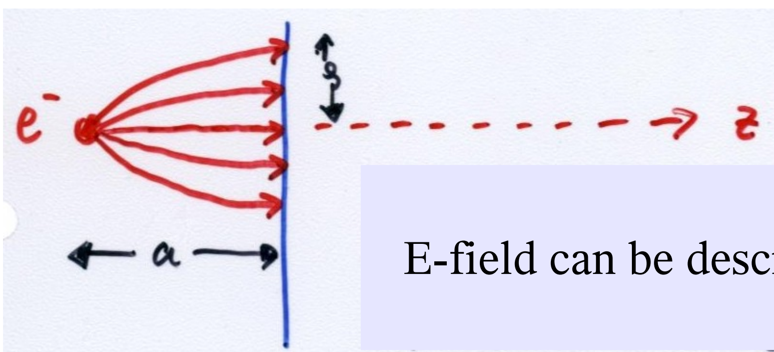

E-field can be described by method of mirror changes

normal component at metal surface
can be generated (Gedankenexperiment) by a dipole

$$|\vec{E}_n| = \frac{a \cdot e}{(a^2+\rho^2)^{3/2}}$$

$$\vec{p} = 2e\vec{a}$$

radiation: annihilation of dipole as particle enters the metal

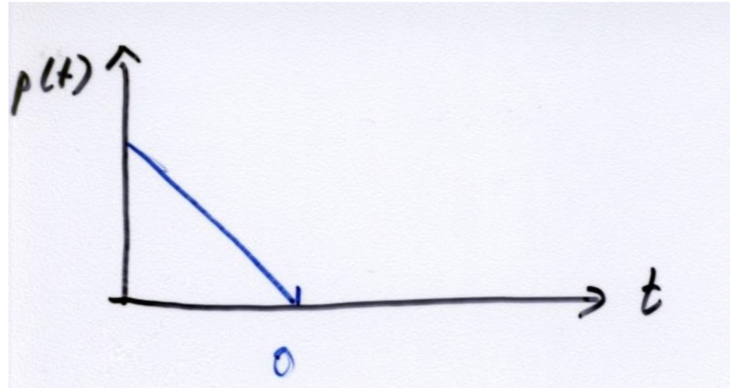

within classical electrodynamics one can show how E-field varies in point $\vec{r}\,' = (\rho', z')$
leading to time dependent polarization

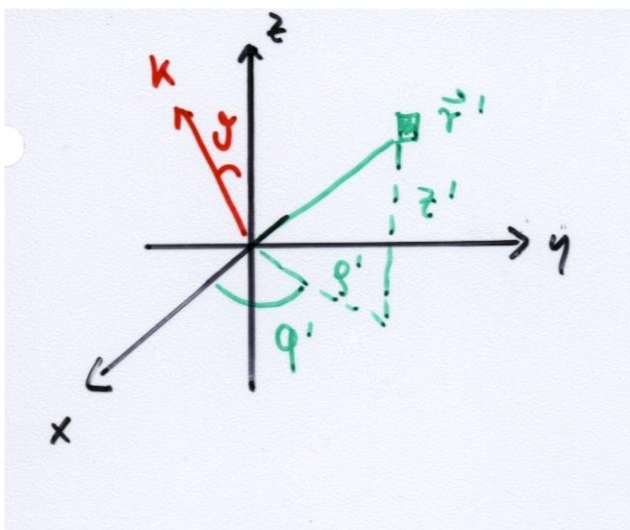

at t = 0 particle is at origin
it propagates in z-dir
consider ratiation in k-dir

$$E_z = \frac{e\gamma(z'-vt)}{(\rho'^2+\gamma^2(z'-vt)^2)^{3/2}}$$

$$E_\perp = \frac{e\gamma\rho'}{(\rho'^2+\gamma^2(z'-vt)^2)^{3/2}}$$

$\rightarrow$ time dependent polarization $\vec{P}(\vec{r}\,', t)$

variation of induced dipoles with time leads to radiation of photons coherent superposition of radiation from neighbouring points in vicinity of track

→ angular range of radiation

ϑ: large Fourrier component of $\vec{\rho}$ at $\rho' \leq \frac{\gamma v}{\omega} \lesssim \rho_{max} \rightarrow \vartheta \simeq 1/\gamma$

→ depth from surface up to which contributions add coherently

formation length $D \cong \gamma \cdot c / \omega_p$

→ volume element producing coherent radiation $V = \pi \rho_{max}^2 D$

characterized by plasma frequency ω_p:

$$\sqrt{\varepsilon_1} = n(\omega) \simeq 1 - \frac{\omega_p^2}{\omega^2} \quad \text{with} \quad \omega_p = \sqrt{\frac{4\pi\alpha n_e}{m_e c^2}} = 28.8\sqrt{\rho \frac{Z}{A}} \text{ eV}$$

typical values: $\omega_p^{CH_2} = 20$ eV $\quad \omega_p^{Luft} = 0.7$ eV

polyethylene

$(\rho \simeq 1\, g/cm^3)$; für $\gamma = 10^3 \rightarrow D \simeq 10\,\mu m$

→ radiator out of foils of this typical thickness; for d > D absorption dominates

typical photon energy: $E_\gamma^{max} \simeq \gamma \hbar \omega_p$ X-rays für $\gamma \gg 1$ $$\frac{d^2W}{d\omega\, d\Omega} = \frac{\alpha}{\pi^2}\left(\frac{\vartheta}{\gamma^{-2}+\vartheta^2+\xi_1^2} - \frac{\vartheta}{\gamma^{-2}+\vartheta^2+\xi_2^2}\right)^2$$

mit $\xi_i = \omega_{pi}^2/\omega^2 = 1-\varepsilon_{1i}(\omega) \ll 1$

→ per boundary

$$\frac{dW}{d\omega} = \frac{\alpha}{\pi}\left(\frac{\xi_1^2+\xi_2^2+2\gamma^{-2}}{\xi_1^2-\xi_2^2}\ln\frac{\gamma^{-2}+\xi_1^2}{\gamma^{-2}+\xi_2^2} - 2\right)$$

foil: contribution from both surfaces,
depending on photon energy interference

typical number of photons per foil ≅ α

→ need many (!) foils
$(O(100)) \rightarrow \langle n_\gamma \rangle = 1\text{-}2$

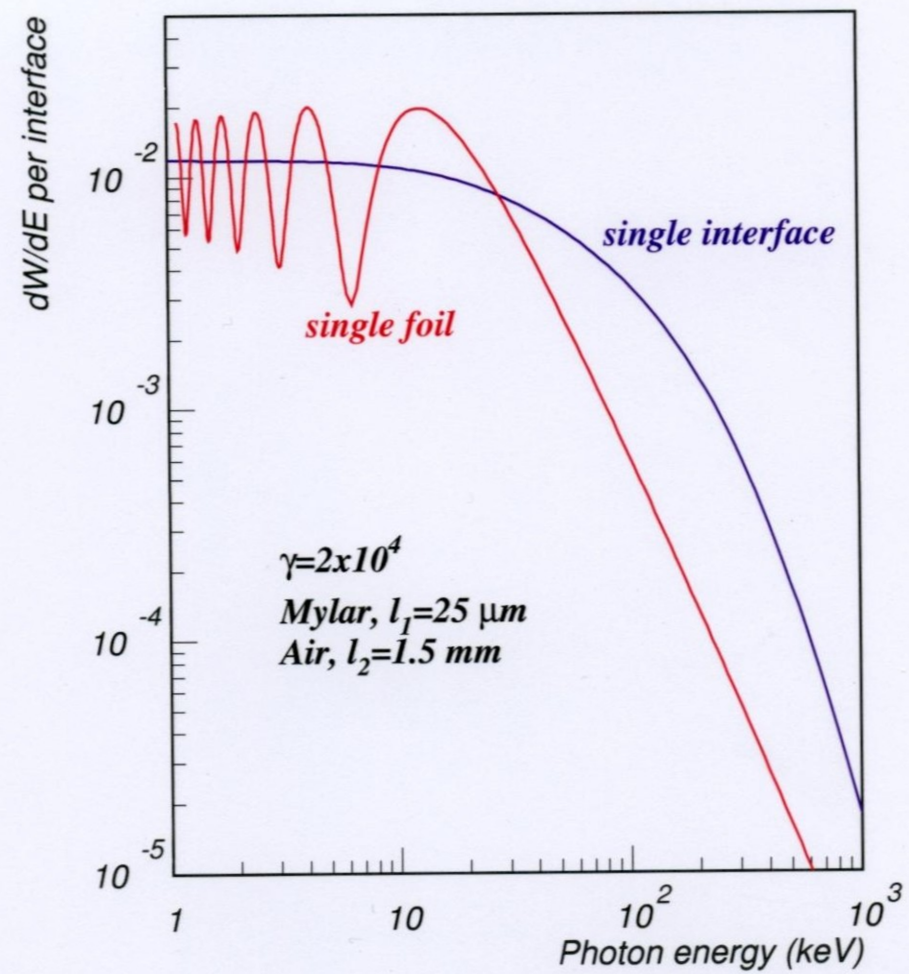

Figure 1: TR spectrum for single interface and single foil configurations.

photons generated in e.g. mylar foils
and absorbed in material (gas) with high Z (xenon)

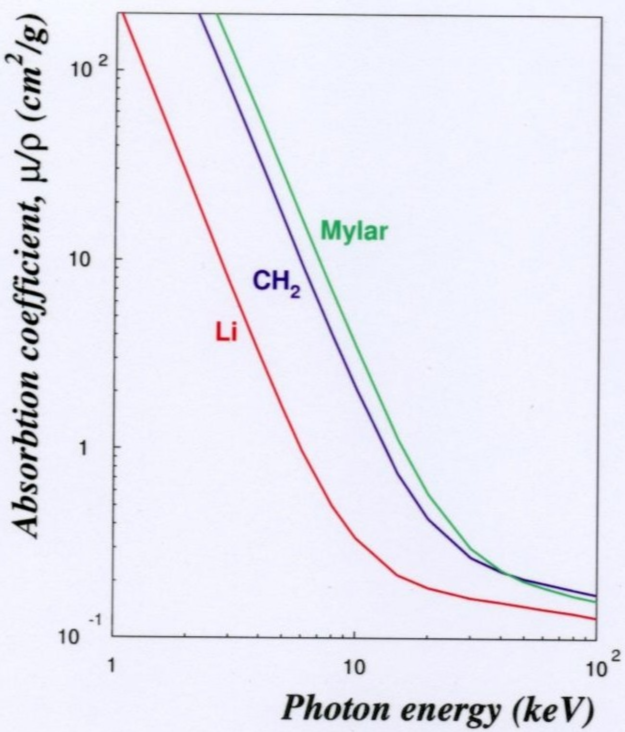

Figure 2: X-rays absorption coefficient for Li, CH_2 and mylar.

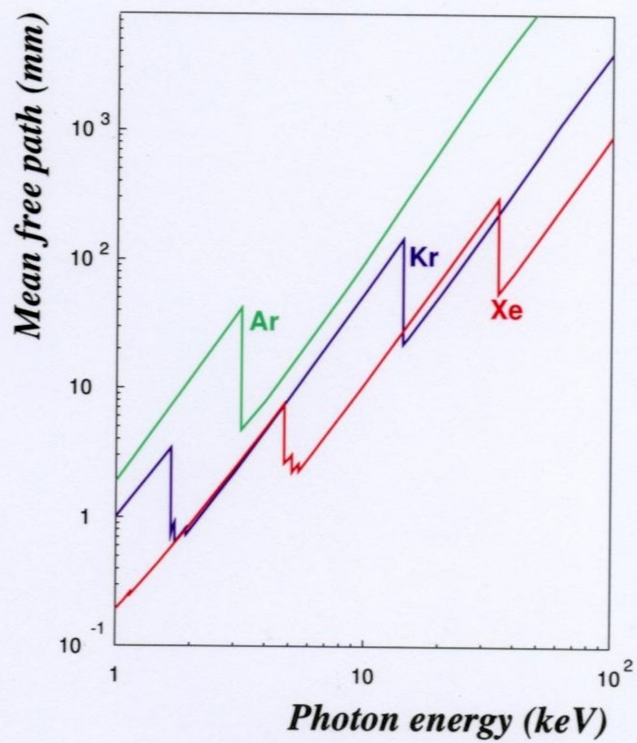

Figure 3: Mean free path of X-rays in different gases.

principle of a transition radiation detector

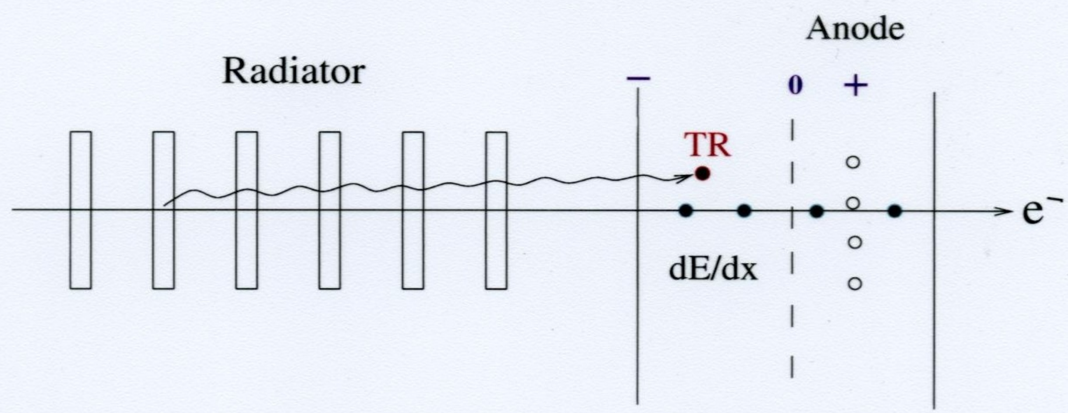

for good absorption prob.
in the detector gas
preferential use of Xe
typical dimension cm

onset of TR photon prod.
in radiator of 100 foils
of thickness d1
in distance d2

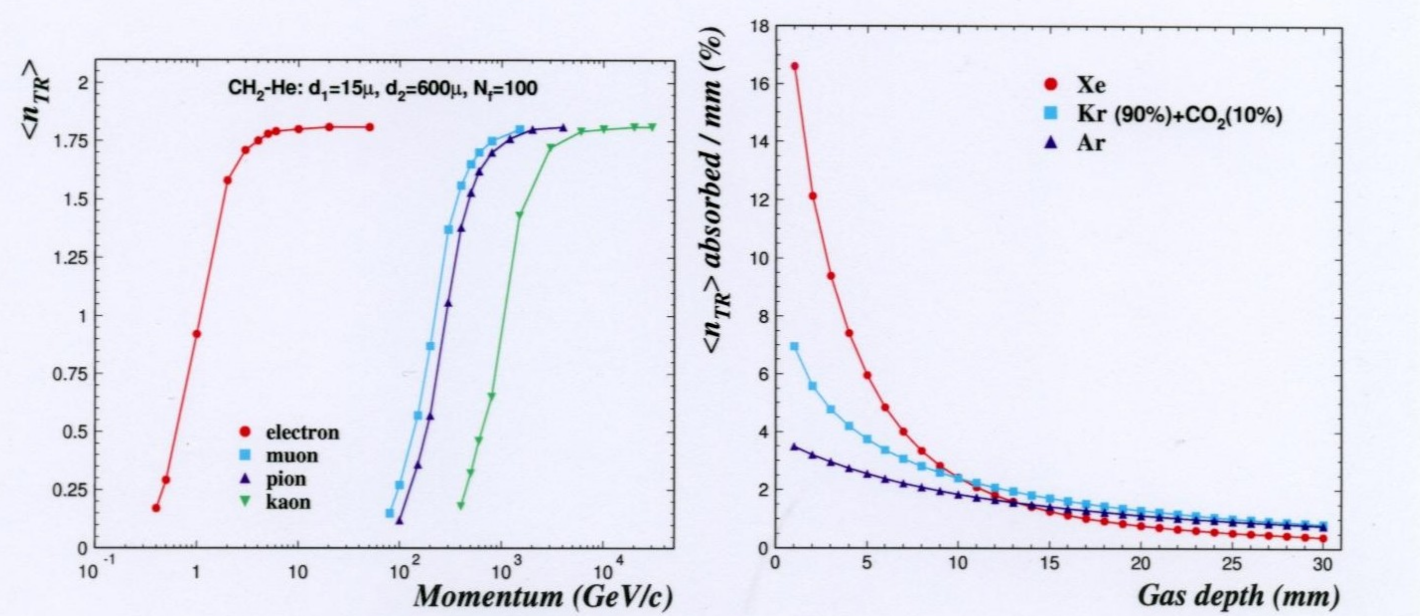

Figure 4: Momentum dependence of TR production for electrons, muons, pions and kaons.

Figure 5: The fraction of absorbed TR photons as a function of detector depth.